

Primordial bispectrum from inflation with background gauge fields

HiroYuki Funakoshi^a and Kei Yamamoto^{a,b}

^aDAMTP, University of Cambridge,
Wilberforce Road, Cambridge, CB3 9AL United Kingdom

^bInstitute of Theoretical Astrophysics, University of Oslo,
P.O. Box 1029, Blindern, N-0315 Oslo, Norway

E-mail: K.Yamamoto@damtp.cam.ac.uk, H.Funakoshi@damtp.cam.ac.uk

Abstract. We study the primordial bispectrum of curvature perturbation in the uniform-density slicing generated by the interaction between the inflaton and isotropic background gauge fields. We derive the action up to cubic order in perturbation and take into account all the relevant effects in the leading order of slow-roll expansion. We first treat the quadratic vertices perturbatively and confirm the results of past studies, while identifying their regime of validity. We then extend the analysis to include the effect of the quadratic vertices to all orders by introducing exact linear mode functions, allowing us to make accurate predictions long after horizon crossing where the features of both the power spectrum and the bispectrum are drastically different. It is shown that the spectra become constant and scale-invariant in the limit of large e-folding. As a result, we are able to impose reliable constraints on the parameters of our theory using the recent observational data coming from Planck.

Keywords: Non-Gaussianity, In-in formalism

Contents

1	Introduction	1
2	Perturbative expansion up to cubic order	4
2.1	Gravity and the scalar field	5
2.2	Gauge field perturbations	6
2.3	Background dynamics and parameters	6
2.4	The cubic action for scalar perturbations	8
2.5	Solving the linear constraints	9
2.6	Curvature of the uniform-density surface	10
3	Analytical estimate of the bispectrum in the limit of small \mathcal{I}	11
3.1	Notations	11
3.2	The outline of the calculation	12
3.3	Summary of the results	13
4	Non-perturbative treatment of the quadratic vertices	16
4.1	Linear evolution equations and their superhorizon solutions	16
4.2	Canonical mode functions	17
4.3	Matching with the de-Sitter mode functions	18
4.4	Estimating the superhorizon contribution to the late-time bispectrum	20
5	Numerical calculation of exact tree-level amplitude	22
5.1	Subhorizon linear evolution and initial conditions	22
5.2	Numerical calculation of the ζ power spectrum	24
5.3	Numerical calculation of the ζ bispectrum	25
6	Implications and concluding remarks	28
A	Details of the perturbative calculation of bispectrum	31
A.1	1-vertex contributions	31
A.2	2-vertex contributions	33
A.3	3-vertex contributions	36
A.4	Second order curvature perturbation and summary	38

1 Introduction

The prediction on the primordial density fluctuation from inflation offers an exciting opportunity to test the physics at high energy that is inaccessible for ground-based experiments. The advent of the Planck satellite, which is expected to improve the constraint on the three-point and higher correlations of the density perturbation at recombination by a factor of 10 to 100, has prompted detailed theoretical investigations into the interaction of the inflaton [1]. So far, the efforts have been focused on the scalar self-interactions and interactions among multiple scalar fields. It is found that single-scalar models with a canonical kinetic term generically predict an undetectable level of non-Gaussian signals [2] while a scalar with

the DBI action or multi-scalar dynamics, such as hybrid inflation or curvaton scenarios, can lead to significant higher-order correlations [3–5]. These models being based on the string theories in their origin of the inflaton, a detection of significant bispectrum or trispectrum can give us a clue for understanding the high-energy physics.

In the context of unified theories of fundamental interactions, however, scalar fields cannot be the only ingredients of the universe. Most of the proposed theories such as superstring theories and M-theory rely on gauge symmetries, and gauge fields are indispensable to mediate interactions among the fields and in some cases to preserve supersymmetries. Even when they are absent in the fundamental Lagrangians, it is a generic prediction of dimensional reduction that a typical scalar field is coupled to some gauge fields [6, 7]. Earlier attempts to drive inflation with vector fields [8–11] turned out to be largely unsuccessful since one needs to abandon gauge symmetries, which results in the introduction of additional degrees of freedom and various instabilities [12–16]. More recently, interactions between the inflaton and gauge fields, motivated by those unified theories of interactions, have been taken into account in the context of preheating [17–22]. In addition to interesting phenomenologies including non-Gaussianity, primordial magnetic fields and gravitational waves [23–32], it was realized that the back reaction of gauge fields on the inflaton can effectively act as an extra friction term so that they slow down the rolling of the scalar field and help causing an accelerated expansion [33–39]. In fact, this back reaction can be so strong that it may generate a significant vacuum expectation value of the gauge fields and violate the isotropy of the universe. On the other hand, there has been a growing interest to maintain a small, but non-vanishing amplitude of classical gauge fields during inflation in order to explain the reported statistical anisotropy of cosmic microwave background radiation (CMBR) in WMAP 7-year [40–42]. By taking into account the aforementioned back reaction classically, the same types of scalar-gauge interactions arising from the high-energy particle theories have been found to enable acceleration of the cosmic expansion without requiring a sufficiently flat potential for the inflaton [43, 44]. This scenario turned out to be free of any classical instabilities or fine-tuning [45–50]. There have also been extensive studies on its potential imprints on CMBR and it was revealed that even a very small amplitude of background energy density of the gauge fields could result in a significant statistical anisotropy in the curvature fluctuation [51–55]. While it implies such an anisotropic vacuum expectation value of gauge fields must be severely constrained, a recent study suggests that their effect on primordial bispectrum is as drastic as its linear counterpart and the resulting non-Gaussianity may still be observable. In another recent development, it has been shown that multiple vector degrees of freedom generically suppress the residual anisotropy of the background space-time through a dynamical attractor mechanism. In particular, when three or more gauge fields are coupled to a scalar field via a common gauge-kinetic function, the final state of the universe is completely isotropic regardless of initial conditions [56]. Such a circumstance may naturally be realized by non-Abelian gauge fields since the equal coupling is guaranteed by the symmetry [57]. There are other instances of isotropic inflation involving non-Abelian gauge fields which also exhibit similar attractor behaviours [58–63]. The linear perturbation of this isotropic inflation with background gauge fields has been studied, which has found that the primordial power spectrum is not strongly constrained by the current observations since the spectrum is perfectly isotropic and almost scale-invariant [64].

In this paper, we investigate the second-order perturbation of an isotropic universe containing three $U(1)$ gauge fields and a scalar inflaton. We compute the bispectrum of curvature perturbation by deploying the in-in formalism and compare the results with the

corresponding work in an anisotropic background [55], which is expected to be qualitatively similar. There are theoretical, phenomenological, and technical reasons for this particular model to be studied:

1. The isotropy maintained by a triad configuration of gauge fields appears to be a generic feature of multiple vector degrees of freedom according to [56]. This model serves as a prototype of the more complicated instances with non-Abelian gauge fields, for which similar features are expected.
2. Because of its isotropy, the model cannot be effectively constrained by the power spectrum. As we anticipate a strong signal in the bispectrum given the analogy to the anisotropic models, it is important to quantify it from a phenomenological point of view.
3. While perturbation around anisotropic backgrounds is extremely involved, one can make a transparent perturbative expansion in the present isotropic model and identify all the relevant contributions.

Besides, it is worth emphasizing that the interactions under discussion frequently appear in supergravity theories that are low-energy effective theories of superstring theories and M-theory. It is therefore of great interest to study observational consequences of these models as they are beyond the reach of any ground-based experiments.

Our results reproduce the previous studies when the e-folding number is relatively small while extending the analysis so that it is applicable to the period long after the horizon exit. A full perturbative expansion of the Lagrangian up to cubic order is carried out and several interaction terms that are not suppressed by any of the slow-roll parameters are identified. We first treat all the interaction terms, both quadratic and cubic, as perturbation and compute the three-point function for the curvature ζ . The amplitude is solely controlled by the parameter \mathcal{I}^2 that represents the ratio of background energy density of the gauge fields to the scalar kinetic energy density. We explicitly show that the leading contribution comes from the vertex involving a scalar field and two gauge fields, which confirms the claim of [55]. The three-point function scales as $\propto \mathcal{I}^2 N_k^3$ where N_k is the e-folding number after horizon exit for a mode with wavenumber k . The shape is local as has been shown in the previous studies. This results in a large f_{NL} when the modification to the power spectrum is assumed to be small. However, we find that this conclusion is valid only if $\mathcal{I}^2 \ll N_k^{-2}$, which is not satisfactory for this isotropic model since \mathcal{I}^2 is not necessarily that small in contrast to the anisotropic cases where this is required to keep the background anisotropy within the range allowed by the observations. A reason for the limited applicability is the quadratic vertices that generate an infinite number of Feynman diagrams in the perturbative expansion even at tree level. In the second half of this paper, we take into account this fact by introducing exact linear mode functions. It turns out that one can solve the linear evolution equations analytically at superhorizon scales. By exploiting their general features, we shall prove that both power spectrum and bispectrum are convergent in the limit $N_k \rightarrow \infty$, determining the late-time value of f_{NL} . In order to obtain more quantitative estimates and handle the intermediate regime, we also solve the linear equations numerically from deep inside the horizon and use them in the integrand of the three-point correlators. We confirm the initial logarithmic behaviours in both power spectrum and bispectrum and their convergence at late times. It turns out that the time evolution of f_{NL} (squeezed) displays some interesting features. It first peaks at $N_k \sim 0.3\mathcal{I}^{-1}$ where the peak value scales as \mathcal{I}^{-1} ; thus for certain

small values of \mathcal{I} , the latest Planck data appear to rule out the possibility of the observable modes in the CMBR arising from this intermediate phase. Then, f_{NL} monotonically decreases and converges to a negative \mathcal{I} -independent constant, $-5/3$.

The paper is organized as follows. In the next section, after sketching the dynamics of the background evolution and introducing relevant parameters, we derive the perturbed Lagrangian up to cubic order. Section 3 gives the detailed procedure of computing the three-point function by perturbative expansion with respect to free de-Sitter mode functions. We calculate all the relevant contributions and identify the leading order term. Section 4 discusses the importance of the deviation from the de-Sitter mode functions on superhorizon scales. In the end we provide estimates for the late-time values for the power spectrum and bispectrum. In section 5, we numerically confirm these analytical results and make the prediction on non-Gaussianity more quantitative. Concluding remarks are given in section 6.

2 Perturbative expansion up to cubic order

Our model contains a scalar field and several gauge fields minimally coupled to gravity:

$$S = \int d^4x \sqrt{-g} \left(\frac{1}{16\pi G} R - \frac{1}{2} \partial_\mu \varphi \partial^\mu \varphi - V(\varphi) - \frac{f(\varphi)^2}{4} F_{\mu\nu}^a F^{a\mu\nu} \right).$$

R is the Ricci scalar curvature and $F_{\mu\nu}^a = \partial_\mu A_\nu^a - \partial_\nu A_\mu^a$; $a = 1, 2, 3$ are three copies of $U(1)$ gauge field strengths. These types of actions have been well studied in the context of magnetogenesis, preheating and anisotropic inflation. It has been realised that the coupling between the scalar field, which is identified to be the inflaton, and gauge fields enables an accelerated phase of expansion even with a relatively steep potential, as we will see later. We note that the energy density of the gauge fields stays constant in the first approximation in the inflating universe, violating the cosmic-no-hair conjecture. It has also been shown that the isotropic configuration of the gauge fields is a dynamical attractor of the system. Based on this result, we study the perturbation of this theory around the isotropic background with a non-vanishing triad of the gauge fields.

We set $8\pi G = 1$ and follow the ADM formalism [65] and parametrize the metric as

$${}^4g_{\mu\nu} = \begin{pmatrix} -N^2 + N_k N^k & N_j \\ N_i & g_{ij} \end{pmatrix}$$

where

$$N^i = g^{ij} N_j, \quad g^{ik} g_{kj} = \delta^i_j.$$

The normalized extrinsic curvature of the constant time slice is given by

$$E_{ij} = -\frac{1}{2} (\dot{g}_{ij} - 2N_{(i|j)})$$

and its intrinsic scalar curvature is

$${}^3R = (g_{ij,kl} + g_{mn} \Gamma_{ij}^m \Gamma_{kl}^n) (g^{ik} g^{jl} - g^{ij} g^{kl}).$$

Electric fields are defined to be

$$E_i^a = F_{0i}^a.$$

2.1 Gravity and the scalar field

The Einstein-Hilbert action in ADM formalism is given by

$$\mathcal{L}_g = \frac{\sqrt{g}}{2N} (E_{ij}E^{ij} - E^2) + \frac{N\sqrt{g}}{2} {}^3R.$$

We assume that the background is a flat Friedmann-Lemaître-Robertson-Walker space-time

$$ds^2 = a(\eta)^2 (-d\eta^2 + \delta_{ij}dx^i dx^j)$$

and write the perturbed metric components as

$$N = a(1 + \phi), \quad N_i = a^2\beta_i, \quad g_{ij} = a^2(\delta_{ij} + 2\gamma_{ij}).$$

When the problem concerns perturbation beyond linear order, one has to be careful in choosing the small quantities with respect to which the order of perturbation is determined. In the present case, we will solve the constraint equations so that ϕ and β_i are expressed in terms of γ_{ij} and the other matter variables. Thus, their order in perturbative expansion is subject to the equations to be solved and we should distinguish different orders as

$$\begin{aligned} \phi &= \phi_{(1)} + \frac{1}{2}\phi_{(2)} + \dots, \\ \beta_i &= \beta_i^{(1)} + \frac{1}{2}\beta_i^{(2)} + \dots. \end{aligned}$$

On the other hand, we avoid a similar expansion for γ_{ij} since it will hardly appear in the following analysis as we are primarily working in the flat gauge, where the perturbation is set to be zero at each order by the choice of gauge. The only exception is the curvature perturbation on the uniform-density slice that will be expanded in terms of the dynamical variables in the flat gauge. As usual, the scalar-vector-tensor decomposition is made in order to decouple the linear-order equations. It is defined by

$$\begin{aligned} \gamma_{ij} &= -\psi\delta_{ij} + E_{,ij} + F_{(i,j)} + \frac{1}{2}h_{ij}, \quad \beta_i^{(n)} = B_{,i}^{(n)} - S_i^{(n)}, \\ S_{i,i}^{(n)} &= F_{i,i} = 0, \quad h_{ii} = 0, \quad h_{ij,j} = 0. \end{aligned}$$

In the uniform-density gauge, we denote the curvature perturbation $-\zeta = \psi$ and expand it as

$$\zeta = \zeta_{(1)} + \frac{1}{2}\zeta_{(2)} + \dots.$$

The 1 + 3 decomposition of the action for the scalar field is given by

$$\mathcal{L}_\varphi = \frac{\sqrt{g}}{2N} \left[\varphi'^2 - 2\varphi'_{,i}N^i + (\varphi_{,i}N^i)^2 \right] - N\sqrt{g} \left[\frac{1}{2}g^{ij}\varphi_{,i}\varphi_{,j} + V(\varphi) \right],$$

where primes denote derivatives with respect to the conformal time η . We split φ into the background and the perturbation:

$$\varphi = \bar{\varphi} + \pi.$$

π will be treated as the dynamical variable in terms of which the perturbative expansion is defined so that we do not need to expand it further.

2.2 Gauge field perturbations

The Maxwell Lagrangian in the ADM formalism reads

$$\mathcal{L}_M = \frac{\sqrt{g}}{2N} f^2 g^{ij} \left(E_i^a + F_{ik}^a N^k \right) \left(E_j^a + F_{jl}^a N^l \right) - \frac{N\sqrt{g}}{4} f^2 g^{ik} g^{jl} F_{ij}^a F_{kl}^a.$$

The perturbative expansion of the vector potentials yields

$$A_0^a = \sigma^a, \quad A_i^a = A(\eta) \delta_i^a + \chi_i^a,$$

where the background quantity $A(\eta)$ behaves effectively as a second scalar field. The background values of A_0^a are taken to be zero by a gauge choice. As in the gravity sector, we should in principle distinguish the different orders of perturbation for the variables that are expanded in terms of the dynamical ones. However, after the adoption of flat slicing and $U(1)$ gauge fixing, we are left only with the dynamical variables from this sector. Hence we suppress this distinction and the scalar-vector-tensor decomposition is carried out as follows:

$$\begin{aligned} \sigma^a &= \mu_{,a} + \nu_a, & \chi_i^a &= \alpha \delta_{ai} + \theta_{,ai} + \epsilon_{aij} (\tau_{,j} + \lambda_j) + \kappa_{(a,i)} + \omega_{ai}, \\ \nu_{i,i} &= \lambda_{i,i} = \kappa_{i,i} = 0, & \omega_{ii} &= 0, & \omega_{ij,j} &= 0. \end{aligned}$$

2.3 Background dynamics and parameters

Before going into the perturbative analysis, we briefly review the background evolution of the system and identify the relevant parameters. The Maxwell's equation can be trivially integrated to give

$$A' = \frac{c}{f^2}$$

where c is an integration constant. As usual, we introduce the "slow-roll" parameters

$$\epsilon_H = 1 - \frac{\mathcal{H}'}{\mathcal{H}^2}, \quad \eta_H = \frac{\epsilon_H'}{\mathcal{H} \epsilon_H}, \quad \left(\mathcal{H} = \frac{a'}{a} \right), \quad (2.1)$$

which characterize the evolution of the scale factor $a(\eta)$. The Raychaudhuri equation

$$2\mathcal{H}' + \mathcal{H}^2 = -\frac{1}{2} \bar{\varphi}'^2 - \frac{c^2}{2a^2 f^2} + a^2 V \quad (2.2)$$

tells that the potential energy has to dominate over the scalar kinetic energy and the energy of gauge fields in order to have an accelerated expansion. This suggests the introduction of another parameter

$$\epsilon_\varphi = \frac{\bar{\varphi}'^2}{2\mathcal{H}^2} \quad (2.3)$$

which controls the evolution of the inflaton. Combined with the Friedmann equation

$$3\mathcal{H}^2 = \frac{1}{2} \bar{\varphi}'^2 + a^2 V + \frac{3c^2}{2a^2 f^2}, \quad (2.4)$$

one derives

$$\frac{c^2}{a^2 f^2} = (\epsilon_H - \epsilon_\varphi) \mathcal{H}^2,$$

which is the representative of the energy density for the gauge fields. Note that $\epsilon_\varphi \leq \epsilon_H$ where equality holds when the gauge fields vanish. Since this deviation from the single-scalar inflation plays a central role, we define the parameter

$$\mathcal{I} = \sqrt{\frac{\epsilon_H - \epsilon_\varphi}{\epsilon_\varphi}}, \quad (2.5)$$

which measures the ratio between the energy density of the gauge fields and the scalar kinetic energy. We note that \mathcal{I} does not have to be small as far as the background dynamics and the power spectrum are concerned. Without loss of generality, we can assume $\bar{\varphi}' > 0$ and use $\bar{\varphi}' = \sqrt{2\epsilon_\varphi}\mathcal{H}$. Now the equation of motion for $\bar{\varphi}$ gives

$$\bar{\varphi}'' = \sqrt{\frac{\epsilon_\varphi}{2}} (2 - 2\epsilon_H + \eta_\varphi) \mathcal{H}^2 \quad (2.6)$$

where

$$\eta_\varphi = \frac{\epsilon'_\varphi}{\mathcal{H}\epsilon_\varphi}. \quad (2.7)$$

In principle, this quantity does not have to be small as long as $\eta_H \ll 1$, but we do assume that it is in order to control the perturbative expansion. Now by differentiating

$$\frac{c^2}{f^2} = (\epsilon_H - \epsilon_\varphi) \mathcal{H}^2 a^2,$$

one obtains

$$\frac{(f^2)_{,\varphi}}{f^2} = -\sqrt{\frac{2}{\epsilon_\varphi}} \left(2 - \epsilon_H + \frac{\epsilon_H \eta_H - \epsilon_\varphi \eta_\varphi}{2(\epsilon_H - \epsilon_\varphi)} \right), \quad (2.8)$$

and using the equation of motion for the scalar field yields

$$\frac{a^2 V_{,\varphi}}{\mathcal{H}^2} = -\frac{1}{\sqrt{2\epsilon_\varphi}} \left(6\epsilon_H - 3\epsilon_H^2 + \epsilon_H \epsilon_\varphi + \frac{3}{2}\epsilon_H \eta_H - \frac{1}{2}\epsilon_\varphi \eta_\varphi \right). \quad (2.9)$$

The first expression tells that the slope of $f(\varphi)$ must be steep in order to maintain the amplitude of gauge fields during inflation. The second implies that the gradient of potential is not necessarily small if $\epsilon_\varphi \ll \epsilon_H$, or equivalently, if $\mathcal{I} \gg 1$. The reason is that the slow roll of the inflaton can be achieved by transferring the scalar kinetic energy to the gauge fields through the coupling $f(\varphi)$. It later turns out that the perturbative approach breaks down when $\mathcal{I} > 1$ anyway, so we assume that $\mathcal{I} < 1$, where the usual intuition from single-scalar model works well. The higher order derivatives of V and f take complicated forms in general, but assuming the constancy of $\eta_{H,\varphi}$ and keeping only the leading-order terms in the small parameters, we obtain

$$\frac{a^2 V_{,\varphi\varphi}}{\mathcal{H}^2} \sim \frac{3\epsilon_H}{2\epsilon_\varphi} (4\epsilon_H - 2\eta_H + \eta_\varphi), \quad (2.10)$$

$$\frac{a^2 V_{,\varphi\varphi\varphi}}{\mathcal{H}^2} \sim \frac{3}{2\sqrt{2\epsilon_\varphi}} \frac{\epsilon_H}{\epsilon_\varphi} (8\epsilon_H \eta_H - 4\epsilon_H \eta_\varphi - 2\eta_H^2 + 3\eta_H \eta_\varphi - \eta_\varphi^2), \quad (2.11)$$

and

$$\frac{(f^2)_{,\varphi\varphi}}{f^2} \sim \frac{8}{\epsilon_\varphi}, \quad \frac{(f^2)_{,\varphi\varphi\varphi}}{f^2} \sim -\left(\frac{8}{\epsilon_\varphi}\right)^{\frac{3}{2}}. \quad (2.12)$$

Finally, we emphasize that this regime of accelerated expansion aided by gauge fields is a dynamical attractor for a wide range of potential and coupling. The readers are referred to ref. [56].

2.4 The cubic action for scalar perturbations

Since the curvature perturbation does not receive any contribution from vector or tensor modes at the linear order, we can eliminate them from the tree-level calculations of three-point correlation functions arising from cubic interactions. Since their power spectra are known to be small, the higher order contribution is expected to be negligible. Hence, we focus on scalar perturbations hereafter.

For the scalar perturbation, the gauge field variables are given by

$$\begin{aligned}\sigma_0^a &= \mu_{,a}, \\ \chi^a_{i} &= \alpha\delta_{ai} + \theta_{,ai} + \epsilon_{aij}\tau_{,j}.\end{aligned}$$

We use the $U(1)$ gauge freedom to set $\theta' + \mu = 0$. It follows that

$$\begin{aligned}\delta F_{ij}^a &= \alpha_{,j}\delta_{ia} - \alpha_{,i}\delta_{ja} + \epsilon_{aik}\tau_{,kj} - \epsilon_{ajk}\tau_{,ki}, \\ \delta E_i^a &= \alpha' + \epsilon_{aij}\tau'_{,j},\end{aligned}$$

where δ indicates the perturbation of the following variables. For the metric, we adopt the flat slicing $\psi = E = 0$. Focusing on scalar modes, we can completely ignore γ_{ij} . The gravitational action drastically simplifies up to cubic order to become

$$a^{-2}\mathcal{L}_g = (1 - \phi_{(1)}) \left[-3\mathcal{H}^2\phi_{(1)}^2 + \frac{1}{2} \left(B_{,ij}^{(1)} B_{,ij}^{(1)} - B_{,ii}^{(1)} B_{,jj}^{(1)} \right) - 2\mathcal{H}\phi_{(1)} B_{,ii}^{(1)} \right].$$

The scalar part is the same as the standard:

$$\begin{aligned}\mathcal{L}_\varphi &= (1 - \phi_{(1)}) \left(\frac{1}{2}\bar{\varphi}^2\phi_{(1)}^2 - \phi_{(1)} (\bar{\varphi}'\pi' + a^2 V_{,\varphi}\pi) - \bar{\varphi}'\pi_{,i} B_{,i}^{(1)} + \frac{1}{2}\pi'^2 - \frac{1}{2}\pi_{,i}\pi_{,i} - \frac{1}{2}a^2 V_{,\varphi\varphi}\pi^2 \right) \\ &\quad - a^2 V_{,\varphi}\phi_{(1)}^2\pi - \pi'\pi_{,i} B_{,i}^{(1)} - \frac{1}{6}a^2 V_{,\varphi\varphi\varphi}\pi^3.\end{aligned}$$

After some straightforward algebra, one obtains the gauge Lagrangian as

$$\begin{aligned}\mathcal{L}_M &= (1 - \phi_{(1)})\mathcal{L}_{MS}^{(2)} - 2f^2\alpha_{,i}B_{,i}^{(1)} \left(\alpha' + \frac{c(f^2)_{,\varphi}}{f^4}\pi \right) + f^2 B_{,i}^{(1)} (\epsilon_{ijk}\alpha_{,j}\tau'_{,k} - \tau_{,ij}\tau'_{,j} - \tau'_{,i}\tau_{,jj}) \\ &\quad + \frac{c^2(f^2)_{,\varphi\varphi\varphi}}{4f^4}\pi^3 + \frac{3c(f^2)_{,\varphi\varphi}}{2f^2}\pi^2\alpha' + (f^2)_{,\varphi}\pi \left(\frac{3}{2}\alpha'^2 - \alpha_{,i}\alpha_{,i} \right) \\ &\quad + (f^2)_{,\varphi}\pi \left(\tau'_{,k}\tau'_{,k} - \frac{1}{2}\tau_{,ij}\tau_{,ij} - \frac{1}{2}\tau_{,ii}\tau_{,jj} \right),\end{aligned}$$

where

$$\begin{aligned}\mathcal{L}_{MS}^{(2)} &= \frac{3c^2}{2f^2}\phi_{(1)}^2 - 3c\phi \left(\alpha' + \frac{c(f^2)_{,\varphi}}{2f^4}\pi \right) - 2c\alpha_{,i}B_{,i}^{(1)} + \frac{3c^2(f^2)_{,\varphi\varphi}}{4f^4}\pi^2 + \frac{3c(f^2)_{,\varphi}}{f^2}\alpha'\pi \\ &\quad + \frac{f^2}{2} (3\alpha'^2 - 2\alpha_{,i}\alpha_{,i} + 2\tau'_{,i}\tau'_{,i} - \tau_{,ij}\tau_{,ij} - \tau_{,ii}\tau_{,jj}).\end{aligned}$$

Therefore, the total Lagrangian up to cubic order is written as

$$\begin{aligned}\mathcal{L} &= (1 - \phi_{(1)})\mathcal{L}^{(2)} - a^4 V_{,\varphi}\phi_{(1)}^2\pi - a^2\pi'\pi_{,i}B_{,i}^{(1)} - 2f^2 \left(\alpha' + \frac{c(f^2)_{,\varphi}}{f^4}\pi \right) \alpha_{,i}B_{,i}^{(1)} \\ &\quad + \left(\frac{c^2(f^2)_{,\varphi\varphi\varphi}}{4f^4} - \frac{1}{6}a^4 V_{,\varphi\varphi\varphi} \right) \pi^3 + \frac{3c(f^2)_{,\varphi\varphi}}{2f^2}\pi^2\alpha' + (f^2)_{,\varphi}\pi \left(\frac{3}{2}\alpha'^2 - \alpha_{,i}\alpha_{,i} \right) \\ &\quad + f^2 (\epsilon_{ijk}\alpha_{,j}\tau'_{,k} - \tau_{,ij}\tau'_{,j} - \tau'_{,i}\tau_{,jj}) B_{,i}^{(1)} + (f^2)_{,\varphi}\pi \left(\tau'_{,k}\tau'_{,k} - \frac{1}{2}\tau_{,ij}\tau_{,ij} - \frac{1}{2}\tau_{,ii}\tau_{,jj} \right),\end{aligned}\tag{2.13}$$

where the quadratic Lagrangian is given by

$$\begin{aligned}
a^{-2}\mathcal{L}^{(2)} = & \left(-3\mathcal{H}^2 + \frac{1}{2}\bar{\varphi}'^2 + \frac{3c^2}{2a^2f^2}\right)\phi_{(1)}^2 + \frac{1}{2}\left(B_{,ij}^{(1)}B_{ij}^{(1)} - B_{,ii}^{(1)}B_{,jj}^{(1)}\right) \\
& - \phi_{(1)}\left(2\mathcal{H}B_{,ii}^{(1)} + \bar{\varphi}'\pi' + \left(a^2V_{,\varphi} + \frac{3c^2(f^2)_{,\varphi}}{2a^2f^4}\right)\pi + \frac{3c}{a^2}\alpha'\right) \\
& - \bar{\varphi}'\pi_{,i}B_{,i}^{(1)} - \frac{2c}{a^2}\alpha_{,i}B_{,i}^{(1)} + \frac{1}{2}\pi'^2 - \frac{1}{2}\pi_{,i}\pi_{,i} - \frac{1}{2}a^2V_{,\varphi\varphi}\pi^2 \\
& + \frac{3c^2(f^2)_{,\varphi\varphi}}{4a^2f^4}\pi^2 + \frac{3c(f^2)_{,\varphi}}{a^2f^2}\alpha'\pi + \frac{f^2}{2a^2}(3\alpha'^2 - 2\alpha_{,i}\alpha_{,i}) \\
& + \frac{f^2}{2a^2}(2\tau'_{,i}\tau'_{,i} - \tau_{,ij}\tau_{,ij} - \tau_{,ii}\tau_{,jj}).
\end{aligned} \tag{2.14}$$

It should be mentioned that we dropped the terms involving $\phi_{(2)}$ and $B^{(2)}$ from the beginning since they multiply the background and linear-order constraint equations, which would be automatically satisfied in our formulation.

2.5 Solving the linear constraints

Using the background equations and parameters, the quadratic Lagrangian can be rewritten as

$$\begin{aligned}
a^{-2}\mathcal{L}^{(2)} = & -a^2V\phi_{(1)}^2 - \mathcal{H}\phi_{(1)}\left(2\nabla^2B^{(1)} + \sqrt{2\epsilon_\varphi}\pi' + \frac{3f}{a}\sqrt{\epsilon_\varphi}\mathcal{I}\alpha'\right) + q_\phi\mathcal{H}^2\phi_{(1)}\pi \\
& + \mathcal{H}B^{(1)}\left(\sqrt{2\epsilon_\varphi}\nabla^2\pi + \frac{2f}{a}\sqrt{\epsilon_\varphi}\mathcal{I}\nabla^2\alpha\right) + \frac{1}{2}\pi'^2 - \frac{1}{2}\pi_{,i}\pi_{,i} \\
& + \frac{f^2}{2a^2}(3\alpha'^2 - 2\alpha_{,i}\alpha_{,i} + 2\tau'_{,i}\tau'_{,i} - \tau_{,ij}\tau_{,ij} - \tau_{,ii}\tau_{,jj}) \\
& - \frac{1}{2}\left(a^2V_{,\varphi\varphi} - \frac{3}{2}(\epsilon_H - \epsilon_\varphi)\frac{(f^2)_{,\varphi}}{f^2}\mathcal{H}^2\right)\pi^2 \\
& - 3\sqrt{2}\frac{f}{a}\mathcal{I}\left(2 - \epsilon_H + \frac{\epsilon_H\eta_H - \epsilon_\varphi\eta_\varphi}{2(\epsilon_H - \epsilon_\varphi)}\right)\mathcal{H}\alpha'\pi
\end{aligned}$$

where we discarded the surface term and defined

$$q_\phi = \frac{1}{\sqrt{2\epsilon_\varphi}}(6\epsilon_\varphi(1 + 2\mathcal{I}^2) - 6\epsilon_H^2 + 4\epsilon_H\epsilon_\varphi + 3\epsilon_H\epsilon_\varphi - 2\epsilon_\varphi\eta_\varphi).$$

Varying $B^{(1)}$ determines $\phi_{(1)}$ as

$$\phi_{(1)} = \sqrt{\frac{\epsilon_\varphi}{2}}\left(\pi + \sqrt{2}\frac{f}{a}\mathcal{I}\alpha\right). \tag{2.15}$$

Using this, variation of $\phi_{(1)}$ leads to

$$\begin{aligned}
\sqrt{\frac{2}{\epsilon_\varphi}}\nabla^2B^{(1)} = & -\pi' + \left(6\mathcal{I}^2 + \frac{\epsilon_\varphi}{2}\mathcal{I}^2(5 + 6\mathcal{I}^2) + \frac{3}{2}\eta_H(1 + \mathcal{I}^2) - \eta_\varphi\right)\mathcal{H}\pi \\
& - \frac{f}{\sqrt{2}a}\mathcal{I}(3\alpha' + (6 - 3\epsilon_H + \epsilon_\varphi)\mathcal{H}\alpha).
\end{aligned} \tag{2.16}$$

These relations will be substituted into the Lagrangian derived in the previous subsection and the curvature perturbation in the uniform-density gauge introduced in the following.

2.6 Curvature of the uniform-density surface

For the purpose of quantum field theory calculations in the multi-field dynamics, the most convenient gauge is the flat gauge where $\gamma_{ij} = h_{ij}$ [3]. However, the observationally relevant quantity is the curvature perturbation in the comoving gauge \mathcal{R}_c that coincides with the curvature in the uniform-density gauge ζ beyond the horizon scale. The latter is more often picked up as done here since it possesses a desirable mathematical property. Hence, we need the transformation law between flat gauge and uniform-density gauge, which we cite from [66] as

$$-\zeta_{(1)} = \mathcal{H} \frac{\delta\rho_{(1)}}{\bar{\rho}'} \quad (2.17)$$

and

$$-\zeta_{(2)} = \frac{\mathcal{H}}{\bar{\rho}'} \left(\delta\rho_{(2)} - \frac{\delta\rho'_{(1)}}{\bar{\rho}'} \delta\rho_{(1)} \right) - \frac{1}{4} \Xi_{kk} + \frac{1}{4} \nabla^{-2} \Xi_{ij,ij} \quad (2.18)$$

where the right-hand sides are evaluated in the flat gauge. We defined the perturbative expansion of the energy density

$$\rho = \bar{\rho} + \delta\rho_{(1)} + \frac{1}{2} \delta\rho_{(2)} + \dots$$

and a quadratic expression

$$\begin{aligned} \Xi_{ij} = & -\frac{2\mathcal{H}}{\bar{\rho}'} \left(\mathcal{H}(1 + 3c_s^2) \left(\frac{\delta\rho_{(1)}^2}{\bar{\rho}'} \right) - \frac{\delta\rho'_{(1)}}{\bar{\rho}'} \delta\rho_{(1)} \right) \delta_{ij} \\ & - \frac{2}{\bar{\rho}'} \left(\delta\rho_{(1),i} B_{,j}^{(1)} + \delta\rho_{(1),j} B_{,i}^{(1)} \right) - \frac{2}{\bar{\rho}'^2} \delta\rho_{(1),i} \delta\rho_{(1),i}. \end{aligned}$$

The background sound speed c_s^2 in the present setting is

$$c_s^2 = \frac{\bar{p}'}{\bar{\rho}'} = -1 + \frac{2}{3} \epsilon_H + \frac{1}{3} \eta_H$$

with \bar{p} being the background pressure. At the linear order, the energy density in the flat gauge is neatly written as

$$a^2 \delta\rho_{(1)} = -6\mathcal{H}^2 \phi_{(1)} - 2\mathcal{H} \nabla^2 B^{(1)}.$$

The background energy density satisfies

$$\bar{\rho} = 3 \frac{\mathcal{H}^2}{a^2},$$

thus

$$\bar{\rho}' = -6\epsilon_H \frac{\mathcal{H}^3}{a^2}.$$

Therefore, the first-order curvature perturbation is given by

$$\zeta_{(1)} = -\frac{1}{3\mathcal{H}\epsilon_H} \left(3\mathcal{H}\phi_{(1)} + \nabla^2 B^{(1)} \right). \quad (2.19)$$

The second-order part will be discussed later.

3 Analytical estimate of the bispectrum in the limit of small \mathcal{I}

In this section, we apply the standard methods of the in-in formalism to the Lagrangian obtained in the previous section. In order to render the problem tractable, we keep only the leading-order contributions in the small parameters $\epsilon_{H,\varphi}, \eta_{H,\varphi}$. An interesting point is that even in the limit of de-Sitter space-time, the key parameter \mathcal{I} does not necessarily vanish. Using equations (2.1) - (2.12) and substituting (2.15) and (2.16), the cubic Lagrangian (2.13) becomes

$$a^{-2}\mathcal{L} = \frac{1}{2}(\pi'^2 - (\nabla\pi)^2) + \frac{f^2}{2a^2}(3\alpha'^2 - 2(\nabla\alpha)^2) + \frac{6\mathcal{I}^2}{\eta^2}\pi^2 + \frac{6\sqrt{2}\mathcal{I}}{\eta}\frac{f}{a}\pi\alpha' \quad (3.1)$$

$$- \frac{4\sqrt{2}\mathcal{I}^2}{\sqrt{\epsilon_\varphi}\eta^2}\pi^3 - \frac{12\mathcal{I}}{\sqrt{\epsilon_\varphi}\eta}\frac{f}{a}\pi^2\alpha' - \sqrt{\frac{2}{\epsilon_\varphi}}\frac{f^2}{a^2}\pi(3\alpha'^2 - 2(\nabla\alpha)^2).$$

We dropped τ for a reason that becomes clear soon. We assume the background is close to de-Sitter, which implies

$$a = -\frac{1}{H\eta}, \quad f = f_0\eta^2 \quad (3.2)$$

and discarded all the terms higher order in slow roll. One can rescale α to set $f_0 = 1$ without loss of generality. We further demand $\mathcal{I} < 1$ since we would like to treat all but kinetic terms perturbatively. The factors of $\sqrt{\epsilon_\varphi}^{-1}$ appearing in the cubic terms might look worrying for the validity of the perturbative approach. But when the action is written in terms of ζ , they are of the same order as the quadratic kinetic terms and the perturbative expansion should be marginally applicable. The following analysis is expected to be valid for $\epsilon_H \ll \mathcal{I} < 1$. We are concerned with the three-point correlation function of the curvature perturbation

$$\zeta_{(1)} = -\frac{\eta}{3\epsilon_H}\sqrt{\frac{\epsilon_\varphi}{2}}\left(\pi' + \frac{3(1+2\mathcal{I}^2)}{\eta}\pi - \frac{3}{\sqrt{2}}H\mathcal{I}\eta^3\alpha'\right), \quad (3.3)$$

which is obtained from (2.19) with (2.15) and (2.16), neglecting all the higher order terms in slow roll. The absence of τ at this linear order justifies its omission from the Lagrangian.

3.1 Notations

We take the free massless part of the action to be the background and treat all the other terms perturbatively. In the interaction picture, we set

$$\pi_I(\eta, \mathbf{x}) = \int \frac{d^3k}{(2\pi)^3} \frac{H}{\sqrt{2k^3}} \left(u_k(\eta) a_{\mathbf{k}} e^{i\mathbf{k}\cdot\mathbf{x}} + u_k^*(\eta) a_{\mathbf{k}}^\dagger e^{-i\mathbf{k}\cdot\mathbf{x}} \right), \quad (3.4)$$

$$\alpha_I(\eta, \mathbf{x}) = \frac{1}{\eta^3} \int \frac{d^3k}{(2\pi)^3} \frac{1}{\sqrt{6c_s^3k^3}} \left(v_k(\eta) b_{\mathbf{k}} e^{i\mathbf{k}\cdot\mathbf{x}} + v_k^*(\eta) b_{\mathbf{k}}^\dagger e^{-i\mathbf{k}\cdot\mathbf{x}} \right), \quad (3.5)$$

where the de-Sitter mode functions are defined to be

$$u_k(\eta) = (i - k\eta)e^{-ik\eta},$$

$$v_k(\eta) = (c_s k\eta - i)e^{-ic_s k\eta}, \quad c_s = \sqrt{\frac{2}{3}}.$$

The interaction Hamiltonian is given by

$$H_I = \frac{6H^2\mathcal{I}^2}{\eta^4} \int d^3w \pi_I^2 + H_I^q + H_I^A + H_I^B + H_I^C$$

where

$$H_I^q = \frac{6\sqrt{2}\mathcal{I}}{H} \int d^3w \pi_I \alpha'_I, \quad H_I^A = \sqrt{\frac{2}{\epsilon_\varphi}} \frac{4\mathcal{I}^2}{H^2 \eta^4} \int d^3w \pi_I^3,$$

$$H_I^B = -\frac{12\mathcal{I}}{\sqrt{\epsilon_\varphi} H} \int d^3w \pi_I^2 \alpha'_I, \quad H_I^C = 3\sqrt{\frac{2}{\epsilon_\varphi}} \eta^4 \int d^3w \pi_I \alpha_I'^2.$$

The term with higher spatial derivatives has been omitted. We often drop the subscript I . Note that it was claimed in [55] that H_I^C gives the leading contribution to the bispectrum. We shall explicitly confirm that it is the case as long as we remain within the regime of validity for the perturbative treatment of the quadratic vertices (i.e. H_I^q and the mass term for π).

We are going to compute the three-point correlation function in Fourier space defined by

$$\langle \zeta(\eta, \mathbf{x}) \zeta(\eta, \mathbf{y}) \zeta(\eta, \mathbf{z}) \rangle = \iiint \frac{d^3k_1}{(2\pi)^3} \frac{d^3k_2}{(2\pi)^3} \frac{d^3k_3}{(2\pi)^3} \langle \zeta_{k_1} \zeta_{k_2} \zeta_{k_3} \rangle (2\pi)^3 \delta(\mathbf{k}_1 + \mathbf{k}_2 + \mathbf{k}_3) e^{i(\mathbf{k}_1 \cdot \mathbf{x} + \mathbf{k}_2 \cdot \mathbf{y} + \mathbf{k}_3 \cdot \mathbf{z})}.$$

We often abbreviate it as $\langle \zeta_k^3 \rangle$.

3.2 The outline of the calculation

Introducing an auxiliary function

$$\xi(\eta, \mathbf{x}) = \pi' + \frac{3}{\eta} \pi, \quad (3.6)$$

the three-point function for ζ can be written as

$$-\frac{54\sqrt{2}\epsilon_H^3}{\sqrt{\epsilon_\varphi^3}} \langle \zeta(\eta, \mathbf{x}) \zeta(\eta, \mathbf{y}) \zeta(\eta, \mathbf{z}) \rangle = \eta^3 \langle \xi(\eta, \mathbf{x}) \xi(\eta, \mathbf{y}) \xi(\eta, \mathbf{z}) \rangle \quad (3.7)$$

$$-\frac{3H\mathcal{I}\eta^6}{\sqrt{2}} (\langle \xi(\eta, \mathbf{x}) \xi(\eta, \mathbf{y}) \alpha'(\eta, \mathbf{z}) \rangle + 2 \text{ perms})$$

$$+\frac{9H^2\mathcal{I}^2\eta^9}{2} (\langle \xi(\eta, \mathbf{x}) \alpha'(\eta, \mathbf{y}) \alpha'(\eta, \mathbf{z}) \rangle + 2 \text{ perms}).$$

Despite the appearance of lower powers of \mathcal{I} in the Lagrangian, the leading-order contribution to $\langle \zeta^3 \rangle$ turns out to be quadratic.¹ Then, the π^2 term in the interaction Hamiltonian is clearly irrelevant. However, we do have to keep H_I^q since it affects, for example $\langle \xi^3 \rangle$ with H_I^B at this

¹This is true for tree-level calculations, but loop contributions may contain terms without any factor of \mathcal{I} .

order. More specifically, $\langle \xi^3 \rangle$ can be written as follows:

$$\langle \xi^3 \rangle = i \int^\eta d\eta_1 \langle [H_I^A(\eta_1), \xi_I^3] \rangle \quad (3.8)$$

$$- \int^\eta d\eta_1 \int^{\eta_1} d\eta_2 \langle [H_I^B(\eta_2), [H_I^q(\eta_1), \xi_I^3]] \rangle \quad (3.9)$$

$$- \int^\eta d\eta_1 \int^{\eta_1} d\eta_2 \langle [H_I^q(\eta_2), [H_I^B(\eta_1), \xi_I^3]] \rangle \quad (3.10)$$

$$- i \int^\eta d\eta_1 \int^{\eta_1} d\eta_2 \int^{\eta_2} d\eta_3 \langle [H_I^C(\eta_3), [H_I^q(\eta_2), [H_I^q(\eta_1), \xi_I^3]]] \rangle \quad (3.11)$$

$$- i \int^\eta d\eta_1 \int^{\eta_1} d\eta_2 \int^{\eta_2} d\eta_3 \langle [H_I^q(\eta_3), [H_I^C(\eta_2), [H_I^q(\eta_1), \xi_I^3]]] \rangle \quad (3.12)$$

$$- i \int^\eta d\eta_1 \int^{\eta_1} d\eta_2 \int^{\eta_2} d\eta_3 \langle [H_I^q(\eta_3), [H_I^q(\eta_2), [H_I^C(\eta_1), \xi_I^3]]] \rangle + O(\mathcal{I}^3). \quad (3.13)$$

In a similar way, $\langle \xi^2 \alpha' \rangle$ contains the quadratic term in the Hamiltonian given as

$$\langle \xi^2 \alpha' \rangle = i \int^\eta d\eta_1 \langle [H_I^B(\eta_1), \xi_I^2 \alpha'_I] \rangle \quad (3.14)$$

$$- \int^\eta d\eta_1 \int^{\eta_1} d\eta_2 \langle [H_I^C(\eta_2), [H_I^q(\eta_1), \xi_I^2 \alpha'_I]] \rangle \quad (3.15)$$

$$- \int^\eta d\eta_1 \int^{\eta_1} d\eta_2 \langle [H_I^q(\eta_2), [H_I^C(\eta_1), \xi_I^2 \alpha'_I]] \rangle + O(\mathcal{I}^2). \quad (3.16)$$

Finally, $\langle \xi \alpha'^2 \rangle$ receives no contribution from the quadratic interaction and becomes

$$\langle \xi \alpha'^2 \rangle = i \int^\eta d\eta_1 \langle [H_I^C(\eta_1), \xi_I \alpha'^2_I] \rangle + O(\mathcal{I}). \quad (3.17)$$

Hence, we have to compute ten distinct integrations to fully work out $\langle \zeta^3 \rangle$ at the quadratic order in \mathcal{I}^2 . We focus on the superhorizon limit of the spectrum, i.e. $-k_i \eta \ll 0$ for all $i = 1, 2, 3$.

3.3 Summary of the results

We list the contributions from each of the ten integrations in the limit of $-k_i \eta \rightarrow 0$. The detailed calculations are presented in the appendix.

1-vertex contributions

$$\begin{aligned} i \int^\eta d\eta_1 \langle [H_I^A(\eta_1), \xi_k^3] \rangle &\rightarrow \sqrt{\frac{2}{\epsilon_\varphi}} \frac{9H^4 \mathcal{I}^2 (k_1^3 + k_2^3 + k_3^3)}{k_1^3 k_2^3 k_3^3 \eta^3} \int^\eta \frac{d\eta_1}{\eta} \cos[(k_1 + k_2 + k_3)(\eta - \eta_1)], \\ i \int^\eta d\eta_1 \langle [H_I^B(\eta_1), \xi_{k_1} \xi_{k_2} \alpha'_{k_3}] \rangle &\rightarrow -\frac{27H^3 \mathcal{I} (k_1^3 + k_2^3)}{\sqrt{\epsilon_\varphi} \eta^6 c_s^3 k_1^3 k_2^3 k_3^3} \int^\eta \frac{d\eta_1}{\eta_1} \cos[(k_1 + k_2 + c_s k_3)(\eta - \eta_1)], \\ i \int^\eta d\eta_1 \langle [H_I^C(\eta_1), \xi_{k_1} \alpha'_{k_2} \alpha'_{k_3}] \rangle &\rightarrow \frac{27H^2}{2\sqrt{2}\epsilon_\varphi \eta^9 c_s^6 k_2^3 k_3^3} \int^\eta \frac{d\eta_1}{\eta_1} \cos[(k_1 + c_s k_2 + c_s k_3)(\eta - \eta_1)]. \end{aligned}$$

2-vertex contributions

$$\begin{aligned}
& - \int^\eta d\eta_1 \int^{\eta_1} d\eta_2 \langle [H_I^B(\eta_2), [H_I^q(\eta_1), \xi_k^3]] \rangle = - \sqrt{\frac{2}{\epsilon_\varphi}} \frac{12H^4 \mathcal{I}^2}{c_s^3 k_1^3 k_2^3 k_3^3 \eta^3} \left(\frac{\mathcal{A}_{2a}}{k_1^3} + 2 \text{ perms} \right), \\
& \mathcal{A}_{2a} \rightarrow 27k_1^3(k_2^3 + k_3^3) \int^\eta \frac{d\eta_1}{\eta_1} \int^{\eta_1} \frac{d\eta_2}{\eta_2} \cos(k_1(\eta - \eta_1)) \cos(c_s k_1(\eta_1 - \eta_2) + (k_2 + k_3)(\eta - \eta_2)), \\
& - \int^\eta d\eta_1 \int^{\eta_1} d\eta_2 \langle [H_I^q(\eta_2), [H_I^B(\eta_1), \xi_k^3]] \rangle = - \sqrt{\frac{2}{\epsilon_\varphi}} \frac{12H^4 \mathcal{I}^2}{c_s^3 k_1^3 k_2^3 k_3^3 \eta^3} \left(\frac{\mathcal{A}_{2b}}{k_1^3} + 2 \text{ perms} \right), \\
& \mathcal{A}_{2b} \rightarrow 27k_1^3(k_2^3 + k_3^3) \int^\eta \frac{d\eta_1}{\eta_1} \int^{\eta_1} \frac{d\eta_2}{\eta_2} \cos((k_1 + k_2)(\eta - \eta_1)) \cos(k_1(\eta - \eta_2) + c_s k_1(\eta_1 - \eta_2)), \\
& - \int^\eta d\eta_1 \int^{\eta_1} d\eta_2 \langle [H_I^C(\eta_2), [H_I^q(\eta_1), \xi_{k_1} \xi_{k_2} \alpha'_{k_3}]] \rangle = \frac{2H^3 \mathcal{I}}{\sqrt{\epsilon_\varphi} c_s^6 k_1^6 k_2^3 k_3^3 \eta^6} \mathcal{B}_{2a} + (1 \leftrightarrow 2), \\
& \mathcal{B}_{2a} \rightarrow 81k_1^3 k_2^3 \int^\eta \frac{d\eta_1}{\eta_1} \int^{\eta_1} \frac{d\eta_2}{\eta_2} \cos(k_1(\eta - \eta_1)) \cos(c_s k_1(\eta_1 - \eta_2) + (k_2 + c_s k_3)(\eta - \eta_2)), \\
& - \int^\eta d\eta_1 \int^{\eta_1} d\eta_2 \langle [H_I^q(\eta_2), [H_I^C(\eta_1), \xi_{k_1} \xi_{k_2} \alpha'_{k_3}]] \rangle = \frac{2H^3 \mathcal{I}}{\sqrt{\epsilon_\varphi} c_s^6 k_1^6 k_2^3 k_3^3 \eta^6} \mathcal{B}_{2b} + (1 \leftrightarrow 2), \\
& \mathcal{B}_{2b} \rightarrow 81k_1^3 k_2^3 \int^\eta \frac{d\eta_1}{\eta_1} \int^{\eta_1} \frac{d\eta_2}{\eta_2} \cos((k_2 + c_s k_3)(\eta - \eta_1)) \cos(c_s k_1(\eta_1 - \eta_2) + k_1(\eta - \eta_2)).
\end{aligned}$$

3-vertex contributions

$$\begin{aligned}
& -i \int^\eta d\eta_1 \int^{\eta_1} d\eta_2 \int^{\eta_2} d\eta_3 \langle [H_I^C(\eta_3), [H_I^q(\eta_2), [H_I^q(\eta_1), \xi_k^3]]] \rangle \\
& \quad = - \sqrt{\frac{2}{\epsilon_\varphi}} \frac{12H^4 \mathcal{I}^2}{c_s^6 k_1^3 k_2^3 k_3^3 \eta^3} (k_3^3 \mathcal{A}_{3a} + 5 \text{ perms}), \\
& \mathcal{A}_{3a} \rightarrow -81k_1^3 k_2^3 k_3^3 \int^\eta \frac{d\eta_1}{\eta_1} \cos(k_1(\eta - \eta_1)) \int^{\eta_1} \frac{d\eta_2}{\eta_2} \cos(k_2(\eta - \eta_2)) \\
& \quad \times \int^{\eta_2} \frac{d\eta_3}{\eta_3} \cos(c_s k_1(\eta_1 - \eta_3) + c_s k_2(\eta_2 - \eta_3) + k_3(\eta - \eta_3)), \\
& -i \int^\eta d\eta_1 \int^{\eta_1} d\eta_2 \int^{\eta_2} d\eta_3 \langle [H_I^q(\eta_3), [H_I^C(\eta_2), [H_I^q(\eta_1), \xi_k^3]]] \rangle \\
& \quad = - \sqrt{\frac{2}{\epsilon_\varphi}} \frac{12H^4 \mathcal{I}^2}{c_s^6 k_1^3 k_2^3 k_3^3 \eta^3} (k_2^3 \mathcal{A}_{3b} + 5 \text{ perms}), \\
& \mathcal{A}_{3b} \rightarrow -81k_1^3 k_2^3 k_3^3 \int^\eta \frac{d\eta_1}{\eta_1} \cos(k_1(\eta - \eta_1)) \int^{\eta_1} \frac{d\eta_2}{\eta_2} \cos(c_s k_1(\eta_1 - \eta_2) + k_2(\eta - \eta_2)) \\
& \quad \times \int^{\eta_2} \frac{d\eta_3}{\eta_3} \cos(k_3(\eta - \eta_3) + c_s k_3(\eta_2 - \eta_3)),
\end{aligned}$$

$$\begin{aligned}
& -i \int^{\eta_1} d\eta_1 \int^{\eta_1} d\eta_2 \int^{\eta_2} d\eta_3 \langle [H_I^q(\eta_3), [H_I^q(\eta_2), [H_I^C(\eta_1), \xi_k^3]]] \rangle \\
& = -\sqrt{\frac{2}{\epsilon_\varphi}} \frac{12H^4\mathcal{I}^2}{c_s^6 k_1^3 k_2^3 k_3^3 \eta^3} (k_2^3 \mathcal{A}_{3c} + 5 \text{ perms}) , \\
\mathcal{A}_{3c} & \rightarrow -81 k_1^3 k_2^3 k_3^3 \int^{\eta_1} \frac{d\eta_1}{\eta_1} \cos(k_1(\eta - \eta_1)) \int^{\eta_1} \frac{d\eta_2}{\eta_2} \cos(c_s k_1(\eta_1 - \eta_2) + k_2(\eta - \eta_2)) \\
& \quad \times \int^{\eta_2} \frac{d\eta_3}{\eta_3} \cos(k_3(\eta - \eta_3) + c_s k_3(\eta_1 - \eta_3)) .
\end{aligned}$$

Note that all of the remaining integrals can be carried out in the limit $-k_i\eta \rightarrow 0$, which result in a logarithm of $-\eta$ for each integration. Therefore, 3-vertex contributions dominate over the others in superhorizon limit, as claimed in [55].

In addition, there is a contribution to bispectrum arising from second- and higher order perturbations of ζ in terms of the field variables π and α . It is evaluated for the second-order term in the appendix and shown to be of order \mathcal{I}^2 , hence subdominant compared to the logarithms from the integrations listed above.

In the end, our result is summarized as follows. At the order of \mathcal{I}^2 , the tree-level amplitude of the three-point function in the super horizon limit becomes

$$\begin{aligned}
\langle \zeta_{k_1} \zeta_{k_2} \zeta_{k_3} \rangle & \rightarrow \frac{3\epsilon_\varphi H^4 \mathcal{I}^2}{2\epsilon_H^3 k_1^6 k_2^6 k_3^6} (k_3^3 \mathcal{A}_{3a} + k_2^3 \mathcal{A}_{3b} + k_1^3 \mathcal{A}_{3c} + 2 \text{ perms}) \\
& \sim \frac{243\epsilon_\varphi H^4 \mathcal{I}^2}{4\epsilon_H^3 k_1^3 k_2^3 k_3^3} (k_1^3 + k_2^3 + k_3^3) (\ln(-K\eta))^3
\end{aligned} \tag{3.18}$$

where K is a reference momentum, say $K = \frac{1}{3}(k_1 + k_2 + k_3)$. While the ambiguity of K arising from the lower limits of the integrations leads to errors of order $\ln(k_i/k_j)$, $i \neq j$, for the wavelengths of interests, this should be of order 10. Since there are many other contributions of similar order which we have already ignored, it does not make sense to overly worry about this reference momentum. As we can see, the bispectrum is of local shape. In order to estimate the f_{NL} in the squeezed limit, which is defined as

$$f_{NL} = \frac{5}{6} \frac{\langle \zeta_{k_1} \zeta_{k_2} \zeta_{k_3} \rangle}{\langle \zeta_{k_1} \zeta_{k_2} \rangle + \langle \zeta_{k_2} \zeta_{k_3} \rangle + \langle \zeta_{k_3} \zeta_{k_1} \rangle} , \tag{3.19}$$

we quote the result from [64] for the power spectrum

$$\langle \zeta_k^2 \rangle \rightarrow \frac{\epsilon_\varphi}{\epsilon_H^2} \frac{H^2}{4k^3} \left(1 + 18\sqrt{6}\mathcal{I}^2 (\ln(-k\eta))^2 \right). \tag{3.20}$$

Under the condition

$$\mathcal{I}^2 \ll 1, \tag{3.21}$$

which implies we can replace ϵ_φ with ϵ_H , we obtain

$$f_{NL} \sim \frac{810\mathcal{I}^2 N_K^3}{(1 + 18\sqrt{6}\mathcal{I}^2 N_K^2)^2}, \tag{3.22}$$

where N_K is the number of efoldings experienced by the relevant modes after horizon crossing. This result qualitatively agrees with the one derived in [55] if the correction term in the denominator is ignored.

However, there are a few unsatisfactory features in this result. The first is the limitation arising from our perturbative approach. Since we are sticking to perturbative expansion in terms of \mathcal{I} , the formula (3.22) can be trusted only for

$$\mathcal{I}^2 (\ln(-K\eta))^2 \ll 1 \quad (3.23)$$

since otherwise we would have to take into account the higher order terms from the Taylor expansion of the denominator. However, the condition (3.23) is much more strict than the generic one (3.21) considering that $N_K = -\ln(-K\eta)$ for the modes relevant in CMBR are of order 50. Namely, the applicability of the analysis so far is limited to $\mathcal{I}^2 \lesssim 10^{-4}$ and we are unable to say anything about f_{NL} for the range $10^{-4} \lesssim \mathcal{I}^2 \lesssim 1$. Furthermore, the fact that $\langle \zeta_k^3 \rangle$ may grow indefinitely as long as inflation continues sounds unpleasant considering the classical stability of the quasi-de-Sitter background. It is distinct from the infrared divergence discussed in [55] which concerns the back reaction of the quantum fluctuations and loop corrections which is beyond the scope of the present article. The divergence is already there at the tree-level calculation. Motivated by this, in the next section, we shall give a more careful analysis on the superhorizon dynamics of the fluctuations.

4 Non-perturbative treatment of the quadratic vertices

It is clear that the above approach based on the perturbative expansion in terms of \mathcal{I} bares a limited applicability even if $\mathcal{I} \ll 1$. From the point of view of the classical stability of this inflationary regime shown in [56], the apparent indefinite growth of the correlation functions after horizon exit should halt sooner or later if all the relevant effects are taken into account. In the Lagrangian (3.1), we have regarded the quadratic interaction terms as perturbative corrections along with the cubic ones. In this way, the proper tree-level amplitude involves an infinite number of Feynman diagrams generated by those quadratic vertices. While we have avoided this issue by focusing on the leading-order contribution in \mathcal{I} , one should expect a convergent result if the higher order corrections are treated appropriately. For this purpose, we investigate the linear perturbation more closely and show that both the power spectrum and the bispectrum become constant in the limit of $\eta \rightarrow 0$ despite the appearance of logarithmic divergence $\ln(-k\eta)$ in the perturbative analysis.

4.1 Linear evolution equations and their superhorizon solutions

The equations of motion at linear order are given by

$$\frac{1}{H^2 \eta^2} (\pi_k'' + k^2 \pi_k^2) - \frac{2}{H^2 \eta^3} \pi_k' - \frac{12\mathcal{I}^2}{H^2 \eta^4} \pi_k = -\frac{6\sqrt{2}\mathcal{I}}{H} \alpha_k' \quad (4.1)$$

$$(3\eta^4 \alpha_k')' + 2k^2 \eta^4 \alpha_k = \frac{6\sqrt{2}\mathcal{I}}{H} \pi_k'. \quad (4.2)$$

It turns out that one can write down analytic expressions for the solutions in the superhorizon limit. Ignoring the spatial gradients, the second immediately integrates to give

$$\alpha_k' = \frac{c_0}{\eta^4} + \frac{2\sqrt{2}\mathcal{I}}{H\eta^4} \pi_k$$

where c_0 is an integration constant. We suppress its k -dependence since there should be no confusion as far as the linear theory is concerned. The same applies to the rest of the

integration constants. Plugging this into the first equation, we derive

$$\pi_k'' - \frac{2}{\eta} \pi_k' + \frac{12\mathcal{I}^2}{\eta^2} \pi_k = -\frac{6\sqrt{2}H\mathcal{I}c_0}{\eta^2}$$

whose general solution can be written as

$$\pi_k = -\frac{H}{\sqrt{2}\mathcal{I}} (c_0 + c_+ (-k\eta)^{p_+} + c_- (-k\eta)^{p_-}) \quad (4.3)$$

with two arbitrary constant c_{\pm} . The power exponents are given by

$$p_{\pm} = \frac{3 \pm \sqrt{9 - 48\mathcal{I}^2}}{2}.$$

The corresponding α is

$$\alpha_k = \frac{c_0}{3\eta^3} + 2(-k)^3 \left(c_1 + \frac{c_+}{p_-} (-k\eta)^{-p_-} + \frac{c_-}{p_+} (-k\eta)^{-p_+} \right) \quad (4.4)$$

with the fourth integration constant c_1 . We used the relations

$$p_{\pm} - 3 = -p_{\mp}.$$

4.2 Canonical mode functions

When the off-diagonal terms in the quadratic Lagrangian are taken into account, the introduction of mode functions is not so straightforward as with independent free fields. In this subsection, we look into the canonical formulation of the field theory. From the Lagrangian (3.1), we read off

$$\hat{\pi} = a\pi \quad \text{and} \quad \hat{\alpha} = \sqrt{3}f\alpha$$

as the canonically normalised field variables. Their conjugate momenta are given by

$$\begin{aligned} \hat{p}_{\pi} &= \hat{\pi}', \\ \hat{p}_{\alpha} &= \hat{\alpha}' + \frac{2\sqrt{6}\mathcal{I}}{\eta} \hat{\pi} \end{aligned}$$

and we impose the canonical commutation relations

$$[\hat{\pi}(\tau, \mathbf{x}), \hat{p}_{\pi}(\tau, \mathbf{y})] = i\delta(\mathbf{x} - \mathbf{y}), \quad [\hat{\alpha}(\tau, \mathbf{x}), \hat{p}_{\alpha}(\tau, \mathbf{y})] = i\delta(\mathbf{x} - \mathbf{y})$$

with all the cross commutators being zero. To diagonalize the Hamiltonian, we introduce the creation and annihilation operators

$$[\hat{a}_{a\mathbf{p}}, \hat{a}_{b\mathbf{q}}^{\dagger}] = \delta_{ab}\delta(\mathbf{p} - \mathbf{q}), \quad a, b = 1, 2$$

and expand the field operators in terms of the mode functions:

$$\begin{aligned} \hat{\pi}(\eta, \mathbf{x}) &= a \sum_{a=1,2} \int \frac{d^3k}{(2\pi)^3} \left(\pi_k^a(\eta) \hat{a}_{a\mathbf{k}} e^{i\mathbf{k}\cdot\mathbf{x}} + \pi_k^{a*}(\eta) \hat{a}_{a\mathbf{k}}^{\dagger} e^{-i\mathbf{k}\cdot\mathbf{x}} \right), \\ \hat{\alpha}(\eta, \mathbf{x}) &= \sqrt{3}f \sum_{a=1,2} \int \frac{d^3k}{(2\pi)^3} \left(\alpha_k^a(\eta) \hat{a}_{a\mathbf{k}} e^{i\mathbf{k}\cdot\mathbf{x}} + \alpha_k^{a*}(\eta) \hat{a}_{a\mathbf{k}}^{\dagger} e^{-i\mathbf{k}\cdot\mathbf{x}} \right). \end{aligned}$$

Here, (π_k^a, α_k^a) , $a = 1, 2$ are two independent solutions of equations (4.1) and (4.2). As an example, for the superhorizon solutions derived in the previous subsection, the mode functions become

$$\pi_k^a = -\frac{H}{\sqrt{2\mathcal{I}}} (c_0^a + c_+^a (-k\eta)^{p_+} + c_-^a (-k\eta)^{p_-}), \quad (4.5)$$

$$\alpha_k^a = \frac{c_0^a}{3\eta^3} + 2(-k)^3 \left(c_1^a + \frac{c_+^a}{p_-} (-k\eta)^{-p_-} + \frac{c_-^a}{p_+} (-k\eta)^{-p_+} \right), \quad (4.6)$$

which are characterized by eight complex constants. In this way, we see that each field operator may excite two different particles. Conversely, for each particle species a , there are two associated mode functions \hat{u}_k^a and \hat{v}_k^a . This simply reflects the fact that the fields themselves do not define particles when there is a quadratic mixing term. This formulation is consistent as long as the mode functions satisfy the following conditions arising from the canonical commutators (from here on, the summation convention for indices a, b, \dots is assumed):

$$\begin{aligned} \pi^a \pi^{a*} - \pi^{a*} \pi^a &= \frac{i}{a^2}, & \alpha^a \alpha^{a*} - \alpha^{a*} \alpha^a &= \frac{i}{3f^2}, \\ \pi^a \alpha^{a*} - \pi^{a*} \alpha^a &= 0, & \pi^a \alpha^{a'} - \pi^{a*} \alpha^{a'} &= 0, \\ \pi^{a'} \alpha^{a*} - \pi^{a*} \alpha^{a'} &= 0, & \pi^{a'} \alpha^{a*} - \pi^{a*} \alpha^{a'} &= \frac{2\sqrt{2}\mathcal{I}}{a^3 f \eta} i. \end{aligned}$$

It can be checked that they are preserved by the evolution equations (4.1) and (4.2) if they are satisfied at an initial time.

Later, it proves to be useful to write down these conditions specifically for the superhorizon mode functions. Those six equations translate into algebraic conditions on the integration constants:

$$c_+^a c_-^{a*} - c_+^{a*} c_-^a = \frac{2i\mathcal{I}^2}{k^3 (p_+ - p_-)}, \quad (4.7)$$

$$c_0^a c_1^{a*} - c_0^{a*} c_1^a = \frac{i}{6k^3}, \quad (4.8)$$

$$c_0^a c_{\pm}^{a*} - c_0^{a*} c_{\pm}^a = c_1^a c_{\pm}^{a*} - c_1^{a*} c_{\pm}^a = 0. \quad (4.9)$$

4.3 Matching with the de-Sitter mode functions

From the solutions (4.3) and (4.4), it is almost obvious that the power spectrum should converge to a constant proportional to $|c_0^a|^2$. In order to estimate its magnitude, however, one needs to determine the constants c_α^a , $\alpha = 0, 1, \pm$ from appropriately initial conditions set deep inside the horizon. As a first approximation, we can match the de-Sitter mode functions:

$$\begin{aligned} \pi_k^a &= \frac{H}{\sqrt{2k^3}} \delta_1^a (i - k\eta) e^{-ik\eta}, \\ \alpha_k^a &= \frac{\eta^{-3}}{\sqrt{6c_s^3 k^3}} \delta_2^a (c_s k\eta - i) e^{-ic_s k\eta} \end{aligned}$$

with the superhorizon counterparts (4.5) and (4.6) at the horizon crossing $k\eta = -1$. We evaluate them and their first derivatives and equate each other. This leads to the following

eight equations:

$$\begin{aligned}
c_0^a + c_+^a + c_-^a &= -\frac{\mathcal{I}\delta_1^a}{\sqrt{k^3}}(1+i)e^i, \\
\frac{c_0^a}{6} + c_1^a + \frac{c_+^a}{p_-} + \frac{c_-^a}{p_+} &= -\frac{\delta_2^a}{\sqrt{24c_s k^3}}\left(1 + \frac{i}{c_s}\right)e^{c_s i}, \\
-c_0^a + (p_+ - 1)c_+^a + (p_- - 1)c_-^a &= \frac{\mathcal{I}\delta_1^a}{\sqrt{k^3}}e^i, \\
-\frac{c_0^a}{6} + 2c_1^a + \frac{p_+ - 1}{p_-}c_+^a + \frac{p_- - 1}{p_+}c_-^a &= \frac{\delta_2^a}{\sqrt{24c_s k^3}}\left(1 + \frac{c_s}{2}i\right)e^{c_s i}.
\end{aligned}$$

These easily solve as

$$\begin{aligned}
c_0^1 &= -\frac{2\mathcal{I}}{\sqrt{k^3}}(1+i)e^i, & c_1^1 &= \frac{\mathcal{I}}{3\sqrt{k^3}}e^i\left(1+i+\frac{3i}{p_+p_-}\right), \\
c_0^2 &= \frac{e^{c_s i}}{2\sqrt{6c_s k^3}}(6+7c_s i), & c_1^2 &= -\frac{e^{c_s i}}{3\sqrt{6c_s k^3}}(3+4c_s i), \\
c_\pm^1 &= \frac{\mathcal{I}}{\sqrt{k^3}}\frac{e^i}{p_\mp - p_\pm}(i+(1+i)p_\mp), & c_\pm^2 &= \frac{p_\mp}{p_\pm - p_\mp}c_0^2.
\end{aligned}$$

We can now estimate the final amplitude of the two-point function. Clearly, the dominant contribution at late time comes from c_0^a s. The mode functions asymptotically approach

$$\pi_k^a(\eta) \sim -\frac{Hc_0^a}{\sqrt{2\mathcal{I}}}, \quad \alpha_k^a(\eta) \sim \frac{c_0^a}{3\eta^3}.$$

Using

$$\zeta = \frac{H\eta^2}{3\epsilon_H}\sqrt{\frac{\epsilon_\varphi}{2}}\left[\hat{\pi}' + \frac{4+6\mathcal{I}^2}{\eta}\hat{\pi} + \sqrt{\frac{3}{2}}\mathcal{I}\left(\hat{\alpha}' - \frac{2}{\eta}\hat{\alpha}\right)\right],$$

we derive

$$\langle \zeta_k^2 \rangle \rightarrow \frac{H^2\epsilon_\varphi}{4\epsilon_H^2\mathcal{I}^2}(1+\mathcal{I}^2)|c_0^a|^2 = \frac{H^2\epsilon_\varphi}{\epsilon_H^2 k^3}(1+\mathcal{I}^2)\left(2 + \frac{103}{144c_s\mathcal{I}^2}\right). \quad (4.10)$$

Although the exact numerical factors should not be trusted due to the errors coming from the matching, the dependence on \mathcal{I}^2 is generic (we will confirm this numerically). The fact that the final amplitude is divergent in the limit small \mathcal{I}^2 might look worrying. But it is also the case in the standard single-scalar inflation where the power spectrum is formally infinite when the background is exactly de-Sitter. The same nature can be seen taking the limit of $\mathcal{I} \rightarrow 0$ and large e-folding number ($-k\eta \rightarrow 0$), rewriting the amplitude of the power spectrum as

$$\langle \zeta_k^2 \rangle \sim O(1)\frac{H^2\epsilon_\varphi}{\mathcal{I}^2\epsilon_H^2 k^3} \sim \frac{H^2}{(\epsilon_H - \epsilon_\varphi)k^3}. \quad (4.11)$$

In the last approximation, we used (2.5) and

$$\mathcal{I} \ll 1 \Leftrightarrow \frac{\epsilon_H}{\epsilon_\varphi} \sim 1.$$

This result is reasonable: the dependence of the power spectrum on the parameters is the same as the single-scalar inflation except that ϵ_φ is now replaced by $\epsilon_H - \epsilon_\varphi$. Recalling that

it represents the energy density of the gauge fields in the unit of H^2 , the power spectrum is inversely proportional to the energy density of the background gauge fields instead of the background scalar kinetic energy. We emphasise that the only approximation we used to derive (4.10) was the matching with de-Sitter mode functions. Hence, we expect the expression is valid even for $\mathcal{I} \gtrsim 1$ in the superhorizon limit.

Comparing the expression (4.10) with the perturbative result (3.20), one can estimate the time when the power spectrum settles down to a constant value after horizon exit. We simply equate these two in the limit of small \mathcal{I} and infer that

$$N_k \sim \mathcal{I}^{-2}. \quad (4.12)$$

Beyond this point, $\langle \zeta_k^2 \rangle$ is conserved as it is in the usual adiabatic perturbation.

4.4 Estimating the superhorizon contribution to the late-time bispectrum

Under the general conditions (4.7) - (4.9) arising from the requirement of canonical commutation relations, one can show that the tree-level amplitude of the three-point function is convergent in the superhorizon limit too.

First of all, let us introduce the mode functions for ζ by

$$\zeta_k^a(\eta) = -\frac{\eta}{3\epsilon_H} \sqrt{\frac{\epsilon_\varphi}{2}} \left(\pi_k^{a'} + \frac{3(1+2\mathcal{I}^2)}{\eta} \pi_k^a - \frac{3}{\sqrt{2}} H \mathcal{I} \eta^3 \alpha_k^{a'} \right), \quad (4.13)$$

whose superhorizon limit becomes

$$\zeta_k^a \rightarrow \frac{H\sqrt{\epsilon_\varphi}}{6\epsilon_H \mathcal{I}} \left[3(1+\mathcal{I}^2) c_0^a(k) + (p_+ + 3) c_+^a(k) (-k\eta)^{p_+} + (p_- + 3) c_-^a(k) (-k\eta)^{p_-} \right]. \quad (4.14)$$

We restored the k -dependence of the coefficients. Now the tree-level amplitude does not involve any multiple integrals and we derive

$$\begin{aligned} \langle \zeta_k^3 \rangle &= i \int^\eta d\eta_1 \langle [H_I^A(\eta_1) + H_I^B(\eta_1) + H_I^C(\eta_1), \zeta_k^3(\eta)] \rangle \\ &= -\sqrt{\frac{2}{\epsilon_\varphi}} \frac{48\mathcal{I}^2}{H^2} \int \frac{d\eta_1}{\eta_1^4} \Im \left(\zeta_{k_1}^{a*}(\eta) \zeta_{k_2}^{b*}(\eta) \zeta_{k_3}^{c*}(\eta) \pi_{k_1}^a(\eta_1) \pi_{k_2}^a(\eta_1) \pi_{k_3}^a(\eta_1) \right) \\ &\quad + \frac{48\mathcal{I}}{\sqrt{\epsilon_\varphi} H} \int d\eta_1 \left[\Im \left(\zeta_{k_1}^{a*}(\eta) \zeta_{k_2}^{b*}(\eta) \zeta_{k_3}^{c*}(\eta) \pi_{k_1}^a(\eta_1) \pi_{k_2}^b(\eta_1) \alpha_{k_3}^{c'}(\eta_1) \right) + 2 \text{ perms} \right] \\ &\quad - 12 \sqrt{\frac{2}{\epsilon_\varphi}} \int d\eta_1 \eta_1^4 \left[\Im \left(\zeta_{k_1}^{a*}(\eta) \zeta_{k_2}^{b*}(\eta) \zeta_{k_3}^{c*}(\eta) \pi_{k_1}^a(\eta_1) \alpha_{k_2}^{b'}(\eta_1) \alpha_{k_3}^{c'}(\eta_1) \right) + 2 \text{ perms} \right]. \end{aligned}$$

Note that

$$\begin{aligned} -\sqrt{\frac{2}{\epsilon_\varphi}} \frac{6\epsilon_H \mathcal{I}^2}{H^2} \zeta_k^{a*}(\eta) \pi_k^a(\eta_1) &= 3(1+\mathcal{I}^2) \left[|c_0^a(k)|^2 + c_0^{a*}(k) c_+^a(k) (-k\eta_1)^{p_+} + c_0^{a*}(k) c_-^a(k) (-k\eta_1)^{p_-} \right] \\ &\quad + (p_+ + 3) \left[c_0^a(k) c_+^{a*}(k) (-k\eta)^{p_+} + |c_+^a(k)|^2 (-k\eta)^{p_+} (-k\eta_1)^{p_+} \right] \\ &\quad + (p_- + 3) \left[c_0^a(k) c_-^{a*}(k) (-k\eta)^{p_-} + |c_-^a(k)|^2 (-k\eta)^{p_-} (-k\eta_1)^{p_-} \right] \\ &\quad + (p_- + 3) c_+^a(k) c_-^{a*}(k) (-k\eta)^{p_-} (-k\eta_1)^{p_+} \\ &\quad + (p_+ + 3) c_+^{a*}(k) c_-^a(k) (-k\eta)^{p_+} (-k\eta_1)^{p_-}. \end{aligned}$$

Because of the conditions (4.9), we have

$$\begin{aligned} \Im(\zeta_k^{a*}(\eta)\pi_k^a(\eta_1)) &= -\sqrt{\frac{\epsilon_\varphi}{2}}\frac{H^2}{6\epsilon_H\mathcal{I}^2}\Im(c_+^a(k)c_-^{a*}(k)) \\ &\times [(p_- + 3)(-k\eta)^{p_-}(-k\eta_1)^{p_+} - (p_+ + 3)(-k\eta)^{p_+}(-k\eta_1)^{p_-}] . \end{aligned} \quad (4.15)$$

Thus, we see that the lowest power of the integrand for the first term must come from

$$\frac{1}{\eta_1^4}\Im(\zeta_{k_1}^{a*}(\eta)u_{k_1}^a(\eta_1))\Re(\zeta_{k_2}^{b*}(\eta)u_{k_2}^b(\eta_1))\Re(\zeta_{k_3}^{c*}(\eta)u_{k_3}^c(\eta_1)) + 2 \text{ perms.}$$

The time dependence of its dominant contribution is given by

$$\eta^{p_-}\eta_1^{p_+-4} \quad \text{or} \quad \eta^{p_+}\eta_1^{p_- -4} ,$$

both of which have the total power of -1 and contain a positive power of η , which implies the integration in the limit $-\eta \rightarrow 0$ is convergent. The bispectrum generated by π^3 vertex long after horizon exit is therefore

$$i \int^\eta d\eta_1 \langle [H_I^A(\eta_1), \zeta_k^3(\eta)] \rangle \sim \frac{\epsilon_\varphi H^4(1+\mathcal{I}^2)^2}{4\epsilon_H^3\mathcal{I}^4} (|c_0^a(k_2)|^2|c_0^a(k_3)|^2 + 2 \text{ perms}) . \quad (4.16)$$

Similarly, using

$$\begin{aligned} -\frac{6\epsilon_H\mathcal{I}\eta_1^4}{H\sqrt{\epsilon_\varphi}}\zeta_k^{a*}(\eta)\alpha_k^{a'}(\eta_1) &= 3(1+\mathcal{I}^2) [|c_0^a(k)|^2 + 2c_0^{a*}(k)c_+^a(k)(-k\eta_1)^{p_+} + 2c_0^{a*}(k)c_-^a(k)(-k\eta_1)^{p_-}] \\ &+ (p_+ + 3) [c_0^a(k)c_+^{a*}(k)(-k\eta)^{p_+} + 2|c_+^a(k)|^2(-k\eta)^{p_+}(-k\eta_1)^{p_+}] \\ &+ (p_- + 3) [c_0^a(k)c_-^{a*}(k)(-k\eta)^{p_-} + 2|c_-^a(k)|^2(-k\eta)^{p_-}(-k\eta_1)^{p_-}] \\ &+ 2(p_- + 3)c_+^a(k)c_-^{a*}(k)(-k\eta)^{p_-}(-k\eta_1)^{p_+} \\ &+ 2(p_+ + 3)c_+^{a*}(k)c_-^a(k)(-k\eta)^{p_+}(-k\eta_1)^{p_-} , \end{aligned}$$

one can show that the second and third integrals give convergent results as

$$i \int^\eta d\eta_1 \langle [H_I^B(\eta_1), \zeta_k^3(\eta)] \rangle \sim -\frac{\epsilon_\varphi H^4(1+\mathcal{I}^2)^2}{\epsilon_H^3\mathcal{I}^4} (|c_0^a(k_2)|^2|c_0^a(k_3)|^2 + 2 \text{ perms}) \quad (4.17)$$

and

$$i \int^\eta d\eta_1 \langle [H_I^C(\eta_1), \zeta_k^3(\eta)] \rangle \sim \frac{5\epsilon_\varphi H^4(1+\mathcal{I}^2)^2}{8\epsilon_H^3\mathcal{I}^4} (|c_0^a(k_2)|^2|c_0^a(k_3)|^2 + 2 \text{ perms}) \quad (4.18)$$

respectively. In the end, the late-time contribution to the three-point function becomes

$$\langle \zeta_k^3 \rangle \sim -\frac{\epsilon_\varphi H^4(1+\mathcal{I}^2)^2}{8\epsilon_H^3\mathcal{I}^4} (|c_0^a(k_1)|^2|c_0^a(k_2)|^2 + |c_0^a(k_2)|^2|c_0^a(k_3)|^2 + |c_0^a(k_3)|^2|c_0^a(k_1)|^2) . \quad (4.19)$$

Assuming the final bispectrum is dominated by the superhorizon contribution, which appears to be the case in the evidence of the numerical study in the next section, one can now estimate the final value of f_{NL} in the squeezed limit $k_1 \ll k_2 \sim k_3$. Note that the dependence of $c_0^a(k)$ on k derived by matching is rather generic. Then, in this limit, we have

$$\langle \zeta_k^3 \rangle \rightarrow -\frac{\epsilon_\varphi H^4(1+\mathcal{I}^2)^2}{4\epsilon_H^3\mathcal{I}^4} |c_0^a(k_1)|^2 |c_0^a(k_2)|^2 . \quad (4.20)$$

Combined with (4.10), the appropriately normalised f_{NL} is computed as

$$f_{NL} \rightarrow -\frac{5}{3} \frac{\epsilon_\varphi}{\epsilon_H} \rightarrow -\frac{5}{3} , \quad (4.21)$$

where the last limit was taken for $\mathcal{I} \rightarrow 0 \Leftrightarrow \epsilon_\varphi \rightarrow \epsilon_H$. This beautiful result will be confirmed in the following section.

5 Numerical calculation of exact tree-level amplitude

Following from the previous section, here we treat the quadratic vertices non-pertubatively with the only difference being that now we calculate most of the contributions numerically. The aim is to negate the need for making any approximations and therefore to make our result more quantitatively accurate. In the analytic results from section 4, we derived the qualitative features of power spectrum and bispectrum by assuming that at horizon crossing the mode functions are those of the free de-Sitter case and applying the superhorizon approximation ($k\eta = 0$) as soon as the mode crosses the horizon ($k\eta = -1$). We have been able to estimate the final amplitude of power spectrum, the time of transition from the perturbative regime discussed in section 3 to the one dictated by the superhorizon mode functions, and calculate the superhorizon contribution to the bispectrum in the limit $k\eta \rightarrow 0$. However, we are yet to have a reliable estimate for the time evolution (or equivalently scale dependence) of the bispectrum.

Here, we calculate the exact mode function, first setting the π and α fields in the Bunch-Davies vacuum deep inside the horizon, solve the coupled linear equations of motion numerically until the modes are far into the superhorizon regime. At this point we switch to using the superhorizon equations of motion and use the analytic solution - this is simply to avoid numerical instabilities encountered in this calculation. Now we only use the analytic superhorizon solution for $-k\eta \ll 1$, so the error introduced by doing so is negligible.

Ultimately, we will be interested in the value of f_{NL} (squeezed) here. Factors of $f_0 H$ present in the Lagrangian (3.1) will be absorbed into the definition of the α field, and the overall multiplicative factor of H^{-2} in front of the Lagrangian will not affect the value of f_{NL} . We therefore set $H = 1$; for quantities such as the power spectrum or bispectrum, reintroducing H will be a matter of an overall multiplicative factor which will be included in the plots. When reintroducing H , \mathcal{I} will need to be replaced with \mathcal{I}/H .

This leaves the factors of ϵ_H and ϵ_φ in the Lagrangian and the definition of the curvature perturbation; in the numerical calculation below, they will be set to 1. It can be easily seen that these two parameters can be reintroduced at the end as an overall multiplicative factor of $\epsilon_H/\epsilon_\varphi = 1 + \mathcal{I}^2$ for the value of f_{NL} computed. The ζ mode functions, power spectrum and bispectrum will need to be multiplied by $H(1 + \mathcal{I}^2)^{-1}\epsilon_\varphi^{-\frac{1}{2}}$, $H^2(1 + \mathcal{I}^2)^{-2}\epsilon_\varphi^{-1}$ and $H^4(1 + \mathcal{I}^2)^{-3}\epsilon_\varphi^{-2}$ respectively, to restore the dependence on these constants.

5.1 Subhorizon linear evolution and initial conditions

Again, the linear equations of motion (4.1) and (4.2) are used, this time keeping the gradient terms. Since the evolution equations do not admit an analytic solution, we will find solutions numerically. For computational convenience, the canonical variables used in this section are π and α , and so their conjugate momenta are given by

$$\begin{aligned} p_\pi &= a^2 \pi' , \\ p_\alpha &= 3a^{-4} \alpha' - 6\sqrt{2}\mathcal{I}\pi . \end{aligned}$$

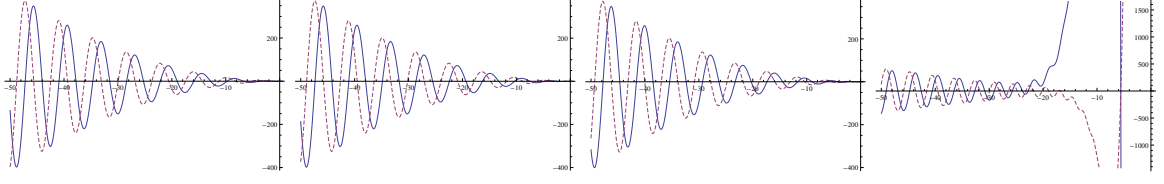


Figure 1. Plots of the ζ_k^1 mode functions during subhorizon, with $k\eta$ along the x -axis. For all plots on this page, the solid line represents the real part and the dashed line represents the imaginary part. The different plots are for different values of \mathcal{I} ; from left to right: $\mathcal{I} = 0.1, 0.5, 1$ and 10 respectively. For smaller values of \mathcal{I} , one can observe the characteristic oscillation and its damping towards horizon exit of de-Sitter mode functions, while the behaviour near the horizon is significantly different for $\mathcal{I} = 10$.

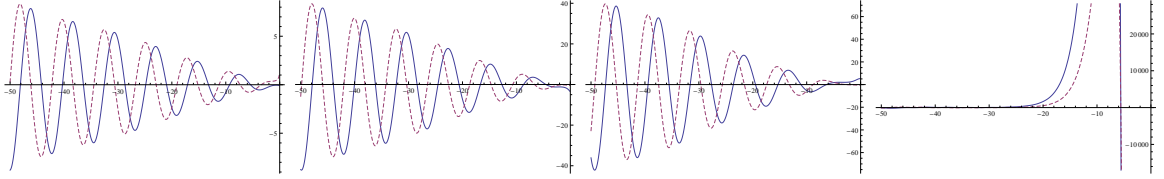


Figure 2. Plots of the ζ_k^2 mode functions during subhorizon, with $k\eta$ along the x -axis. The subhorizon dynamics appears to be similar between ζ_k^1 and ζ_k^2 .

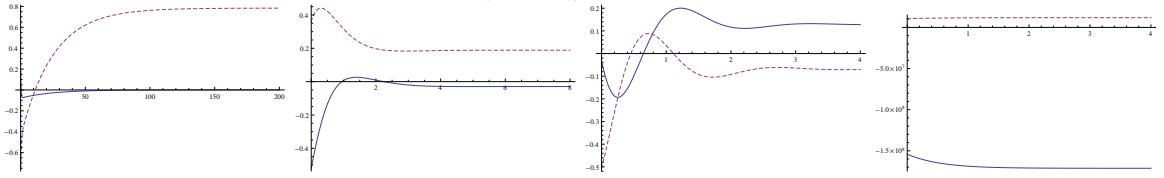


Figure 3. Plots of the ζ_k^1 mode functions during superhorizon, with cosmic time $(-\ln(-k\eta))$ along the x -axis. While the evolution of individual mode functions significantly depends on the value of \mathcal{I} , all of them settle down to constant in agreement with the analytical results.

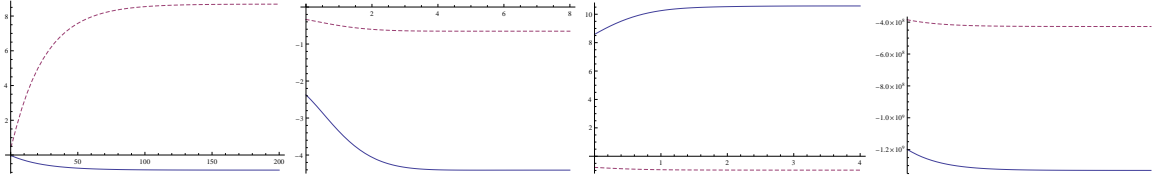


Figure 4. Plots of the ζ_k^2 mode functions during superhorizon, with cosmic time along the x -axis. On superhorizon scales, ζ_k^1 and ζ_k^2 evolve differently.

The initial conditions for the mode functions are given by the Bunch-Davies condition, expressed here in terms of the canonical variables for each k mode as:

$$\pi^a = \frac{\delta_1^a}{\sqrt{2k^3}}(i - k\eta)e^{-ik\eta}, \quad p_\pi^a = \delta_1^a a^2 \sqrt{\frac{k}{2}} i \eta e^{-ik\eta}, \quad (5.1)$$

$$\alpha^a = \frac{\delta_2^a}{\sqrt{6c_s^3 k^3}}(c_s k \eta^{-2} - i \eta^{-3})e^{-ic_s k \eta}, \quad (5.2)$$

$$p_\alpha^a = \frac{3\delta_2^a}{a^4 \sqrt{6c_s^3 k^3}}(-ic_s^2 k^2 \eta^{-2} - 3c_s k \eta^{-3} - 3i \eta^{-4})e^{-ic_s k \eta}. \quad (5.3)$$

The point here is that these are the conditions required on the mode functions for the fields to

be in the Bunch-Davies vacuum deep inside the horizon, and for the canonical commutation relations to hold. Given the definitions of the conjugate momenta, the initial conditions for solving the linear evolution equations will then be given by (5.1) and (5.2) along with

$$\alpha_k^{a'} = \frac{\delta_2^a}{\sqrt{6c_s^3 k^3}} (-ic_s^2 k^2 \eta^{-2} - 3c_s k \eta^{-3} - 3i\eta^{-4}) e^{-ic_s k \eta} + \frac{2\mathcal{I} \delta_1^a}{\sqrt{k^3}} (-k\eta^{-3} + i\eta^{-4}) e^{-ik\eta} \quad (5.4)$$

in place of (5.3) for some $-k\eta \gg 1$. For the results in this section, the initial conditions for the modefunctions were set at $(\eta)_{\text{init}} = -1000$.

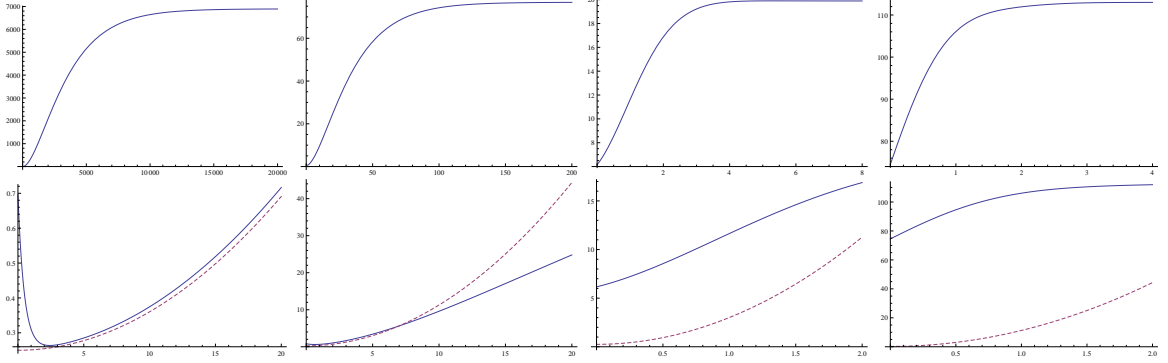


Figure 5. Time evolution for the power spectrum $\langle \zeta_k^2 \rangle$. The first line represents the time evolution until the power spectrum becomes constant and the second line represents the time evolution for a some time after horizon crossing, both plotted against cosmic time. The second line provides a comparison between the perturbative result from [56] and the numerical results from section 5 for the time evolution of $\langle \zeta_k^2 \rangle$, with the numerical results in solid lines and the analytic ones in dashed lines. From left to right: $\mathcal{I} = 0.01, 0.1, 0.5$ and 1 . While the analytical results fit the initial growth fairly well for $\mathcal{I} = 0.01, 0.1$, the discrepancy is significant for larger \mathcal{I} or late time.

5.2 Numerical calculation of the ζ power spectrum

Now we calculate the power spectrum for the curvature perturbation. A similar analysis has been carried out in [52], so the results in this section are to recap these results, and to verify that these results are consistent with the perturbative expression for the curvature power spectrum [56]. Using the π and α mode functions we are able to define the ζ mode function as

$$\zeta_k^a = -\frac{\eta}{3\sqrt{2}} \left(\pi_k^{a'} + \frac{3(1+2\mathcal{I}^2)}{\eta} \pi_k^a - \frac{3}{\sqrt{2}} H \mathcal{I} \eta^3 \alpha_k^{a'} \right), \quad (5.5)$$

and hence

$$\langle \zeta_k^2 \rangle = \zeta_k^a \zeta_k^a. \quad (5.6)$$

The ζ mode functions are plotted in figures 1, 2, 3 and 4, while the numerical and analytic results for the power spectrum are shown in figures 5, 6 and 7. The perturbative solution for the time evolution of $\langle \zeta_k^2 \rangle$ is shown to be useful only for small \mathcal{I} (figure 5), while the analytic estimate for the final value of the power spectrum, derived in section 4, is valid for values of \mathcal{I} up to around 0.2 (figure 7). The lack of quantitative agreement beyond $\mathcal{I} \sim 0.2$ is presumably due to the error arising from the matching since for larger values of \mathcal{I} , the numerical calculations (figures 1, 2, 3, 4) show a significant deviation from the de-Sitter

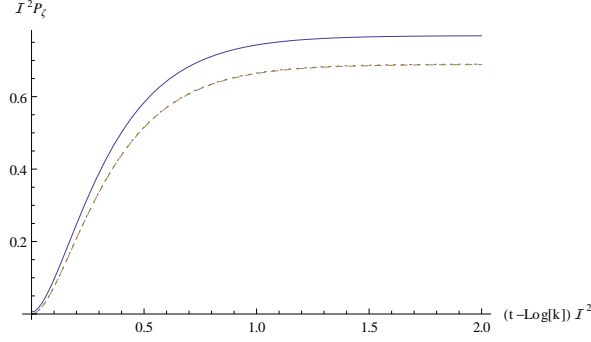


Figure 6. Time evolution of $\langle \zeta_k^2 \rangle$ rescaled according to analytic expectation; the (overlapping) dotted and dashed lines are $\mathcal{I} = 0.001$ and 0.01 , and the solid line is $\mathcal{I} = 0.1$. The time coordinate has been rescaled by \mathcal{I}^2 and the power spectrum amplitude by \mathcal{I}^2 . It clearly indicates the time of transition to the constant regime $-\ln(-k\eta) \sim \mathcal{I}^{-2}$.

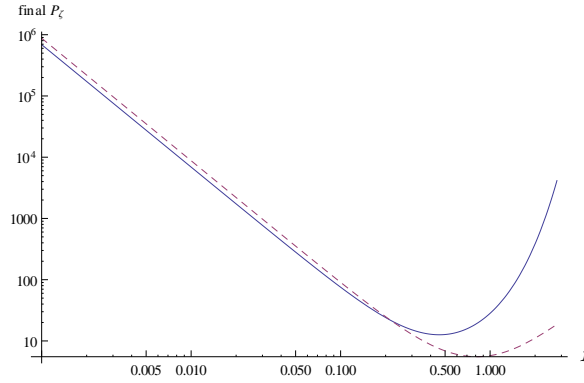


Figure 7. Values for the power spectrum $\langle \zeta_k^2 \rangle$ after settling down to a constant, plotted as a function of \mathcal{I} . The solid line represents the numerical result, and the dotted line represents the analytic expression from section 4. There is a good agreement for $\mathcal{I} \lesssim 0.2$.

mode functions around horizon crossing. The characteristic timescale for the time evolution for $\langle \zeta_k^2 \rangle$ before it reaches constant is shown to be \mathcal{I}^{-2} for $\mathcal{I} \lesssim 0.1$, in agreement with the analytical estimate (4.12) from the previous section (figure 6). This result has a significant implication on the validity of the perturbative treatment of quadratic vertices discussed at the end of section 3. The transition to constant regime occurs around

$$N_k \sim \mathcal{I}^{-2} \quad (5.7)$$

which is much later than the time at which the correction term to the power spectrum becomes comparable to the leading-order term $N_k \sim \mathcal{I}^{-1}$. In fact, the numerical evidence suggests that the perturbative formula (3.20) is valid right up to $\mathcal{I}^2 \lesssim N_k^{-1}$, or for CMBR scale ($N_k \sim 50$), $\mathcal{I} \lesssim O(0.1)$. This observation plays a key role in imposing the observational constraint from Planck later.

5.3 Numerical calculation of the ζ bispectrum

By solving the coupled linear evolution equations, we in effect include the contribution from the infinitely many tree-level Feynman diagrams coming from the quadratic H^q term, and hence obtain a result correct to all orders in \mathcal{I} (provided loop contributions are negligible).

Therefore, the exact tree-level amplitude for the bispectrum, by standard application of Wick's theorem, is given by

$$\begin{aligned} \langle \zeta_{k_1} \zeta_{k_2} \zeta_{k_3} \rangle = & -48\sqrt{2}\mathcal{I}^2 \int^\eta \frac{d\eta_1}{\eta_1^4} \Im \left(\zeta_{k_1}^{a*}(\eta) \zeta_{k_2}^{b*}(\eta) \zeta_{k_3}^{c*}(\eta) \pi_{k_1}^a(\eta_1) \pi_{k_2}^b(\eta_1) \pi_{k_3}^c(\eta_1) \right) \\ & + 48\mathcal{I} \int^\eta d\eta_1 \Im \left(\zeta_{k_1}^{a*}(\eta) \zeta_{k_2}^{b*}(\eta) \zeta_{k_3}^{c*}(\eta) \pi_{k_1}^a(\eta_1) \pi_{k_2}^b(\eta_1) \alpha_{k_3}^{c'}(\eta_1) + 2 \text{ perms} \right) \\ & - 12\sqrt{2} \int^\eta d\eta_1 \eta_1^4 \Im \left(\zeta_{k_1}^{a*}(\eta) \zeta_{k_2}^{b*}(\eta) \zeta_{k_3}^{c*}(\eta) \pi_{k_1}^a(\eta_1) \alpha_{k_2}^{b'}(\eta_1) \alpha_{k_3}^{c'}(\eta_1) + 2 \text{ perms} \right). \end{aligned}$$

In particular, we now only have to compute 1-vertex terms.

The evaluation of the integrand turns out to be a numerically unstable process sufficiently far outside the horizon, requiring a very precise cancellation of terms. It therefore becomes impractical to carry out the calculation with the numerically solved mode functions beyond a certain point. To overcome this difficulty, for $-k\eta < 10^{-5}$ we switch to using the analytic superhorizon solution discussed in the previous section. The only difference is in the matching of the analytic superhorizon solution; here we evaluate the numerical mode functions (and their time derivative) at $-k\eta = 10^{-5}$ and use these as the matching conditions for the analytic superhorizon solution. Then, for $-k\eta < 10^{-5}$ the time integrals in the above expression are computed analytically, therefore avoiding the problem of numerical instabilities. When performing the first stage of this computation (the numerical stage), we employ the technique recently developed in [67]. As we will see later, the bispectrum (or more precisely, the shape function) is peaked in the squeezed limit, and therefore to concentrate on the salient features we will restrict most of our analysis to the squeezed limit.

We start by crosschecking our numerical calculations against the perturbative results from section 3 (figure 8), for small \mathcal{I} ($= 10^{-3}$) for sometime after horizon exit where the perturbative treatment of the quadratic vertex H^q is justified. This underwrites the overall consistency between the analytical and numerical methods.

In figure 9, we confirm the convergence of the bispectrum generated by each cubic vertex. As one can see, while H^C is the dominant contribution in the perturbative regime as it grows the fastest $(\ln(-k\eta))^3$, it is overtaken by H^B when the perturbative approximation breaks down. It also exhibits an approximate \mathcal{I}^{-4} scaling of the final value of bispectrum, which is equivalent to the \mathcal{I} independence of f_{NL} that was inferred at the end of the previous section. The characteristic timescale for the transition to constant is again shown to be \mathcal{I}^{-2} .

From the $(\ln(-k\eta))^3$ perturbative growth in the bispectrum, one may expect that the superhorizon contribution to the bispectrum dominates over the subhorizon contribution; in figure 10 we verify that this is indeed the case for most values of \mathcal{I} . The bispectrum is evaluated at $\eta = 0$, and the $k\eta < -1$ (subhorizon) and $k\eta > -1$ (superhorizon) contributions to the time integral are plotted separately as a function of \mathcal{I} . The two become comparable only as \mathcal{I} reaches order unity, and for $\mathcal{I} \lesssim 0.1$ the subhorizon contribution is negligible.

In figure 11, we plot the intermediate time evolution of f_{NL} , with the numerical calculation on the left panel and perturbative result on the right. For $N_k \ll \mathcal{I}^{-1}$, the power spectrum is essentially constant and f_{NL} grows as N_k^3 . When $N_k \gtrsim 0.1\mathcal{I}^{-1}$, the power spectrum starts to be overtaken by the correction term and scale as N_k^2 , which results in the peak around $N_k \sim 0.3\mathcal{I}^{-1}$. The maximum value appears to scale as \mathcal{I}^{-1} , which means it may well be observable for a small value of \mathcal{I} . Since these peaks occur on timescales $\propto \mathcal{I}^{-1}$, the time dependence (and therefore scale dependence) of f_{NL} around this maximum can be understood by the perturbative results where analytical expressions are available.

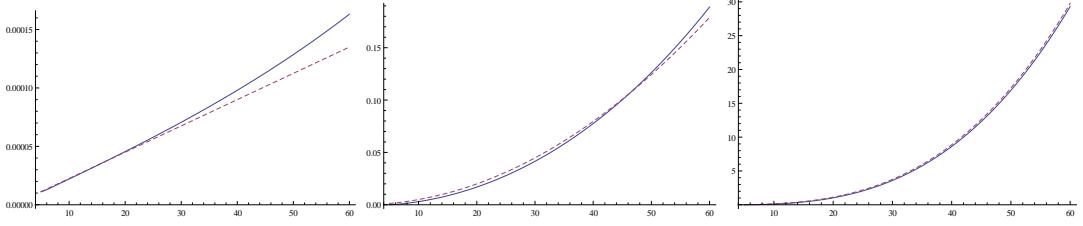


Figure 8. Comparison between the analytic (perturbative) and numerical values of the bispectrum in the squeezed limit, for $\mathcal{I} = 0.001$ just after horizon crossing, showing a very good agreement; from left to right are the contributions from H^A , H^B and H^C respectively, with the numerical value in solid lines and analytic in dashed lines. For all the results in this section, the squeezed limit is evaluated by taking the bispectrum in the configuration $k_1 \times 10^2 = k_2 = k_3$.

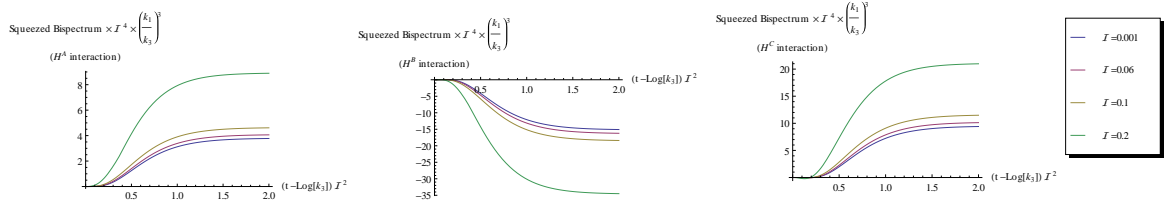


Figure 9. Late-time evolution of the bispectrum in the squeezed limit. There are two properties here which cannot be seen from the perturbative calculation; the contribution to the bispectrum from the second vertex becomes negative, and the contribution from all three vertices become constant after some number of e-folds $\sim \mathcal{I}^{-2}$. For small \mathcal{I} , the final value of the squeezed bispectrum exhibits a \mathcal{I}^{-4} scaling.

However, for later times $\gtrsim \mathcal{I}^{-2}$ this is no longer the case, with f_{NL} turning negative; this behaviour is shown in figure 12, where we plot the late-time evolution of f_{NL} in the squeezed limit for different values of \mathcal{I} . The final convergent value appears to be $-5/3$ independent of \mathcal{I} , in agreement with the results of the previous section. It is also seen in figure 13 where the final value is presented as a function of \mathcal{I} . We suspect that the cause of irregular behaviour for $\mathcal{I} \gtrsim 0.1$ is due to the significant contribution from the subhorizon evolution. We also note that given that there are two scalar degrees of freedom here, the single-field consistency relation [2] does not hold.

We conclude this section by mentioning a few words about the shape of the bispectrum. As can be seen from figure 13, the bispectrum is peaked in the squeezed limit, which is expected given the fact that it is predominantly determined by the superhorizon evolution which tends to generate local bispectra. Provided that we wait until all relevant modes have become constant (as done for the plot), it is perfectly scale-invariant too. This can be understood by noting that since the background geometry is de-Sitter and the interaction terms are de-Sitter invariant, the correlation functions for the perturbations which have become constant are scale-invariant; in particular, for the modes which have settled down to the final value, both the power spectrum and the bispectrum are scale-invariant. By similar arguments, where we have plotted the time evolution of any quantity such as f_{NL} , they can be used to read off the scale dependence at any given time.

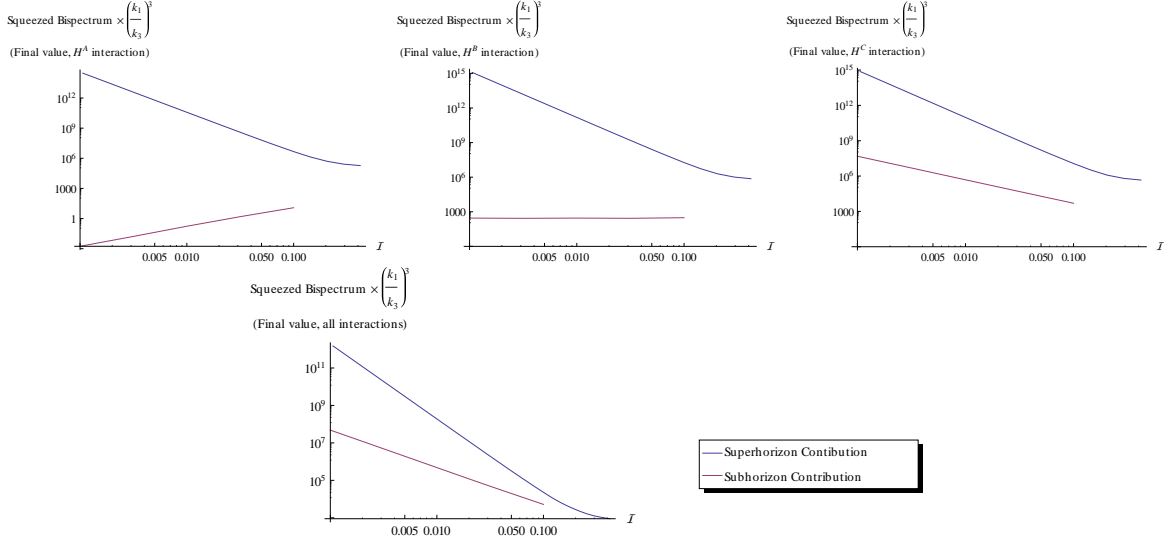


Figure 10. Relative importance of the subhorizon and superhorizon contributions to the final value of the squeezed bispectrum. As \mathcal{I} approaches 1, the subhorizon and superhorizon contributions become comparable. For the plots of the H^B interaction and combined interactions, the negative of the bispectrum was taken for the purposes of taking a log plot. We were unable to obtain reliable results for the subhorizon contribution for $\mathcal{I} \gtrsim 0.1$, so they were not included in the above plots.

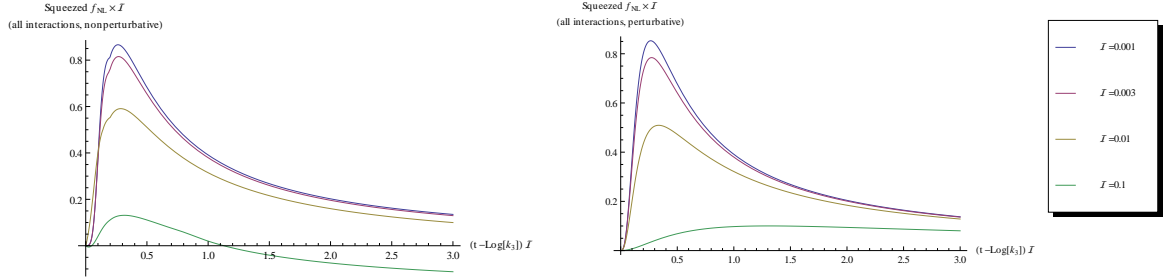


Figure 11. Intermediate time evolution of f_{NL} in the squeezed limit for $\mathcal{I} = 0.001, 0.003, 0.01$ and 0.1 . f_{NL} first grows as N_k^3 and eventually peaks around $N_k \sim 0.3/\mathcal{I}$. The peak value appears to be $\sim \mathcal{I}^{-1}$. Then it monotonically decays until eventually settling down to a negative constant. The behaviour of the peak, at least for $\mathcal{I} \lesssim 0.01$, can be understood perturbatively since the timescale for the peaking of f_{NL} is smaller than that of the breakdown of perturbation theory.

6 Implications and concluding remarks

We have studied the perturbation of a model of inflation where a stable isotropic phase of inflation is realized by a scalar field coupled with a triplet of Abelian gauge fields. We derived the general action for scalar perturbation up to cubic order and identified all the relevant terms in the limit of vanishing slow-roll parameters. Using the standard method of in-in formalism, we first treated both the quadratic and cubic vertices perturbatively and computed the bispectrum at the leading order in the expansion parameter \mathcal{I} . The resulting expression was consistent with the previous studies and f_{NL} in the squeezed limit was shown

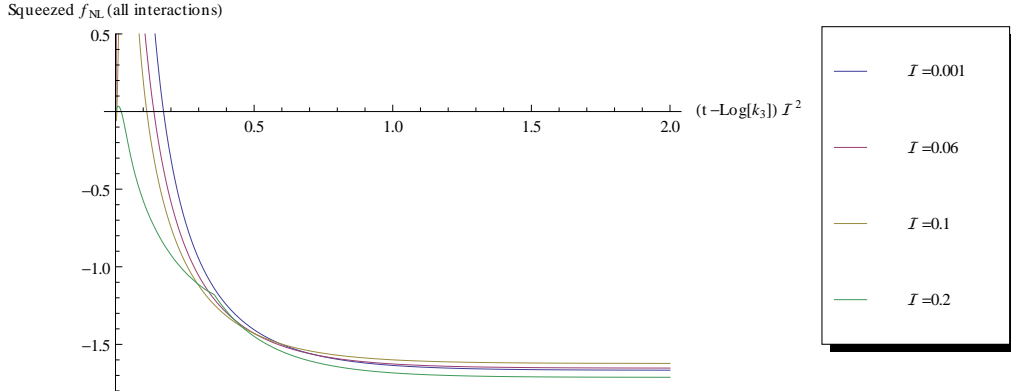


Figure 12. Late time evolution of f_{NL} in the squeezed limit for $\mathcal{I} = 0.001, 0.06, 0.1$ and 0.2 . The x-axis is e-folding number after horizon crossing rescaled by \mathcal{I}^2 , showing the characteristic timescale for f_{NL} to become constant. The final value is independent of \mathcal{I} .

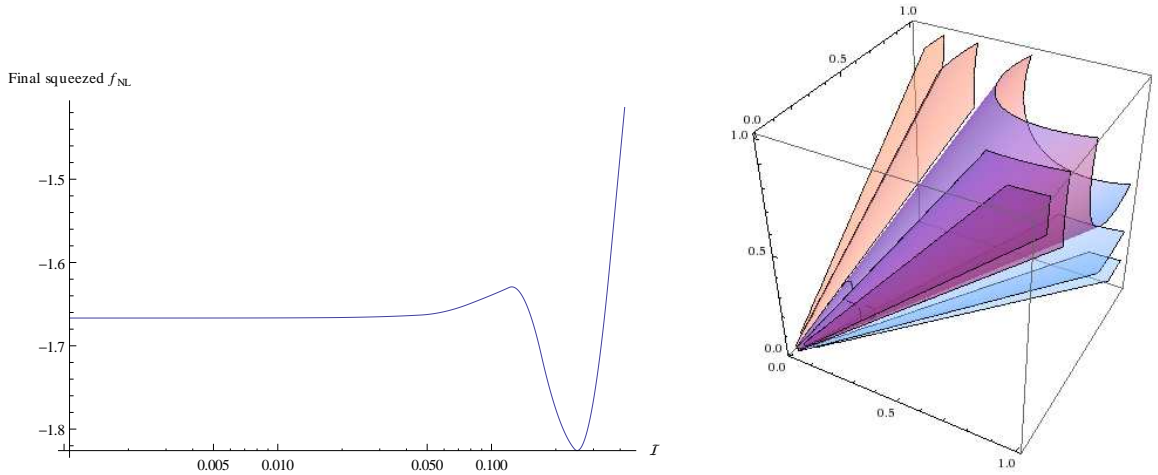


Figure 13. Left: the final value of f_{NL} in the squeezed limit, at least for $\mathcal{I} \lesssim 0.1$, is independent of \mathcal{I} appearing to take the value $-\frac{5}{3}$. Right: The shape of bispectrum for $\mathcal{I} = 0.01$, final value. What is plotted here are contours for $(k_1 k_2 k_3)^2 B(k_1, k_2, k_3)$, with the three axes being k_1 , k_2 and k_3 . It is peaked in the squeezed limit and is scale-invariant.

to be proportional to $\mathcal{I}^2 N_k^3$ where N_k is the e-folding number after the relevant modes exit the horizon. We then pointed out the limited applicability of this approach even for $\mathcal{I} \ll 1$ and rectified it by introducing the exact linear mode functions which take into account the effect of the infinite number of tree-level diagrams generated by the quadratic vertices. Solving the linear evolution equations analytically in the superhorizon limit, we proved that both the power spectrum and the bispectrum are convergent in the limit $N_k \rightarrow \infty$, with the late-time bispectrum being local in shape.

In order to obtain a more quantitative estimate of the bispectrum and f_{NL} , we carried

out an extensive numerical analysis employing in part the recently developed technique [67]. We confirmed the analytical results and found a number of interesting features. In calculating the time evolution of f_{NL} in the squeezed limit, we find that it peaks at some characteristic time after horizon crossing, with this peak value scaling as \mathcal{I}^{-1} . After peaking, it settles down to the same value (independent of \mathcal{I} for small \mathcal{I}) as was estimated analytically: $f_{NL} = -\frac{5}{3}$.

We now discuss the implications of our calculations. Recent Planck [68] data suggest f_{NL} should be of order unity. The modes observable in our Universe typically experience around 50 e-folds after horizon crossing and we already argued that the perturbative expression (3.22) is valid as long as $\mathcal{I} \lesssim 0.1$. Thus excluding $f_{NL} > 10$, we can constrain \mathcal{I} to satisfy either $\mathcal{I}^2 \lesssim 10^{-7}$ or $\mathcal{I}^2 \gtrsim 10^{-3}$. For $\mathcal{I} \gtrsim 0.1$, our numerical calculations suggest that f_{NL} is in the constant regime for $N_k \sim 50$ and its value is of order unity (left panel in figure 13).

We first emphasise that our analysis here is complete at tree-level. It indicates the overall consistency of this model in the classical regime; any fluctuations present at horizon crossing remain bounded and so do their correlation functions (at the very least at the 2-point and 3-point level). For a certain range of values of \mathcal{I} , the model is ruled out by the latest observational constraint on f_{NL} by Planck. However, for large values of \mathcal{I} approaching 1, the length scales currently observable would come from the late-time stage where f_{NL} is of order unity and hence within Planck bounds. Similarly, for small \mathcal{I} , f_{NL} grows sufficiently slowly after horizon crossing and will remain within current observational constraints.

One can expect that the same qualitative features will also apply to the anisotropic models where the background is permeated by one or two gauge fields with non-vanishing vacuum expectation values. The difference is that there the vector fields also contribute to the spatial anisotropy and there is a strict upper bound for \mathcal{I} . It is going to be difficult to repeat our analysis for anisotropic models since the consistent perturbative expansion requires the inclusion of vector and tensor modes which are coupled to the scalars through the background anisotropy. For this purpose, it would be interesting to look into the relation between our results and the delta- N formalism [69]. In fact, the isotropic case can be regarded as a particular two-scalar model and the formalism should apply without any problem. Since the convergence of the power spectrum and bispectrum is based on the superhorizon evolution, the delta- N formalism will reproduce them in a more elegant manner. Since its mathematical basis resides in the equivalence of the superhorizon curvature perturbation to the background evolution of the FLRW universe [70], an appropriate extension to anisotropic backgrounds sounds plausible and can be a powerful tool to handle the complicated interactions among different modes.

Another important theoretical issue is consistency of the quantum field theory in the existence of background gauge fields. The authors of [55] claimed that the infrared contribution of the one-loop diagrams can be interpreted as the rescaling of the background vacuum expectation value of the gauge fields so as to take into account the quantum mechanically created modes that froze in outside the horizon. Although we have not discussed this issue in the present article, it will be certainly an interesting direction of further research.

Finally, it is in principle straightforward to extend our analysis to inflationary models with non-Abelian gauge fields, either the one based on gauge-kinetic coupling [47, 57] or Chern-Simons coupling [60]. Given the qualitative similarity between Abelian and non-Abelian models when all the vertices are treated perturbatively, it is natural to expect that a similar convergent result in the limit of large e-folding can be established, although it is mathematically far from obvious. From a phenomenological point of view, it would be important to clarify the difference among different scenarios so that one is able to observationally

distinguish between them.

Acknowledgments

We would like to thank Xingang Chen, Misao Sasaki and Jiro Soda for useful comments and Federico Urban for interesting discussions. KY is also grateful to the support and hospitality of the Institute of Theoretical Astrophysics in the University of Oslo where a part of this work was completed.

A Details of the perturbative calculation of bispectrum

Here, we give the details of the integrations and handling of second-order perturbations necessary for determining the leading-order bispectrum (3.18). First of all, let us introduce the following mode functions:

$$\begin{aligned}\xi(\tau, \mathbf{x}) &= \int \frac{d^3k}{(2\pi)^3} \frac{H}{\sqrt{2k^3}\eta} \left(g_k(\eta) a_{\mathbf{k}} e^{i\mathbf{k}\cdot\mathbf{x}} + g_k^*(\eta) a_{\mathbf{k}}^\dagger e^{-i\mathbf{k}\cdot\mathbf{x}} \right), \\ \alpha'(\eta, \mathbf{x}) &= \int \frac{d^3k}{(2\pi)^3} \frac{1}{\sqrt{6c_s^3 k^3} \eta^4} \left(h_k(\eta) b_{\mathbf{k}} e^{i\mathbf{k}\cdot\mathbf{x}} + h_k^*(\eta) b_{\mathbf{k}}^\dagger e^{-i\mathbf{k}\cdot\mathbf{x}} \right), \\ g_k(\eta) &= [i(3 + k^2\eta^2) - 3k\eta] e^{-ik\eta}, \\ h_k(\eta) &= [i(3 - c_s^2 k^2\eta^2) - 3c_s k\eta] e^{-ic_s k\eta}.\end{aligned}$$

It will be useful later to note that

$$g_k^*(\eta) u_k(\tilde{\eta}) = (3 + k^2\eta(\eta + 3\tilde{\eta}) - 3ik(\eta - \tilde{\eta}) + ik^3\eta^2\tilde{\eta}) e^{ik(\eta - \tilde{\eta})}, \quad (\text{A.1})$$

$$h_k^*(\eta) v_k(\tilde{\eta}) = (-3 + c_s^2 k^2\eta(\eta - 3\tilde{\eta}) + 3ic_s k(\eta - \tilde{\eta}) + ic_s^3 k^3\eta^2\tilde{\eta}) e^{ic_s k(\eta - \tilde{\eta})}. \quad (\text{A.2})$$

A.1 1-vertex contributions

Let us start from the single integration (3.8). One can easily go to Fourier space and derive

$$\begin{aligned}\langle \xi_k^3 \rangle &= i \sqrt{\frac{2}{\epsilon_\varphi}} \frac{4\mathcal{I}^2}{H^2\eta^3} \frac{H^6}{8k_1^3 k_2^3 k_3^3} \int^\eta \frac{d\eta_1}{\eta_1^4} 6 (u_{k_1} u_{k_2} u_{k_3} g_{k_1}^* g_{k_2}^* g_{k_3}^* - g_{k_1} g_{k_2} g_{k_3} u_{k_1}^* u_{k_2}^* u_{k_3}^*) \\ &= -\sqrt{\frac{2}{\epsilon_\varphi}} \frac{6\mathcal{I}^2 H^4}{k_1^3 k_2^3 k_3^3 \eta^3} \int^\eta \frac{d\eta_1}{\eta_1^4} \Im (g_{k_1}^*(\eta) g_{k_2}^*(\eta) g_{k_3}^*(\eta) u_{k_1}(\eta_1) u_{k_2}(\eta_1) u_{k_3}(\eta_1)).\end{aligned}$$

At a first glance, the integral looks divergent as $\eta \rightarrow 0$ even if the factor of η^3 in (3.7) is taken into account. However, it is not the case since we have

$$\Im (g_{k_1}^*(\eta) g_{k_2}^*(\eta) g_{k_3}^*(\eta) u_{k_1}(\eta) u_{k_2}(\eta) u_{k_3}(\eta)) = 9 (k_1^3 + k_2^3 + k_3^3) \eta^3 + O(\eta^5).$$

Therefore, an integration by parts gives

$$\begin{aligned}\mathcal{A}_1 &= \int^\eta \frac{d\eta_1}{\eta_1^4} \Im (g_{k_1}^*(\eta) g_{k_2}^*(\eta) g_{k_3}^*(\eta) u_{k_1}(\eta_1) u_{k_2}(\eta_1) u_{k_3}(\eta_1)) \\ &= -3(k_1^3 + k_2^3 + k_3^3) + O(\eta^2) + \frac{1}{3} \int^\eta \frac{d\eta_1}{\eta_1^3} \Im (g_{k_1}^* g_{k_2}^* g_{k_3}^* (u_{k_1} u_{k_2} u_{k_3})').\end{aligned}$$

The same type of cancelation of power holds for the remaining integrals. It is also helped by the fact that

$$u'_k(\eta) = ik^2\eta e^{-ik\eta},$$

which is a manifestation of the constancy after horizon exit of the de-Sitter mode functions. Repeating another integration by parts, we are left with

$$\begin{aligned} \mathcal{A}_1 &= 6(k_1^3 + k_2^3 + k_3^3) + O(\eta^2) \\ &+ \frac{1}{3} \int \frac{d\eta_1}{\eta_1} k_1^3 \Im \left(g_{k_1}^*(\eta) g_{k_2}^*(\eta) g_{k_3}^*(\eta) e^{-ik_1\eta_1} u_{k_2}(\eta_1) u_{k_3}(\eta_1) \right) + 2 \text{ perms} \\ &- \frac{1}{3} \int d\eta_1 \Im \left(g_{k_1}^* g_{k_2}^* g_{k_3}^* k_1^2 e^{-ik_1\eta_1} \left(k_2^2 e^{-ik_2\eta_1} u_{k_3} + k_3^2 e^{-ik_3\eta_1} u_{k_2} \right) \right) + 2 \text{ perms}. \end{aligned}$$

The third line is finite. The leading contribution is logarithmically divergent in η as

$$\langle \xi_k^3 \rangle \rightarrow \sqrt{\frac{2}{\epsilon_\varphi}} \frac{9H^4 \mathcal{I}^2 (k_1^3 + k_2^3 + k_3^3)}{k_1^3 k_2^3 k_3^3 \eta^3} \int^\eta \frac{d\eta_1}{\eta_1} \cos [(k_1 + k_2 + k_3) (\eta - \eta_1)].$$

The cross correlations (3.14) and (3.17) are in principle similar. We have

$$\begin{aligned} \langle \xi_{k_1} \xi_{k_2} \alpha'_{k_3} \rangle &= \frac{24\mathcal{I}}{\sqrt{\epsilon_\varphi} H \eta^6} \frac{H^4}{4k_1^2 k_2^2} \frac{1}{6c_s^3 k_3^3} \Im \left(g_{k_1}^*(\eta) g_{k_2}^*(\eta) h_{k_3}^*(\eta) T_{k_3}(\eta) \right), \\ T_{k_1}(\eta) &= \int^\eta \frac{d\eta_1}{\eta_1^4} h_{k_1}(\eta_1) u_{k_2}(\eta_1) u_{k_3}(\eta_1). \end{aligned}$$

and

$$\begin{aligned} \langle \xi_{k_1} \alpha'_{k_2} \alpha'_{k_3} \rangle &= -\sqrt{\frac{2}{\epsilon_\varphi}} \frac{6}{\eta^9} \frac{H^2}{2k_1^3} \frac{1}{36c_s^6 k_2^3 k_3^3} \Im \left(g_{k_1}^*(\eta) h_{k_2}^*(\eta) h_{k_3}^*(\eta) H_{k_1}(\eta) \right), \\ H_{k_1}(\eta) &= \int^\eta \frac{d\eta_1}{\eta_1^4} u_{k_1}(\eta_1) h_{k_2}(\eta_1) h_{k_3}(\eta_1). \end{aligned}$$

In carrying out these integrals, it is useful to note that

$$\frac{1}{\eta^4} h_k = \left(\frac{v_k}{\eta^3} \right)'. \quad (\text{A.3})$$

It will be later useful to derive the explicit forms of T_k and H_k . Straightforward integrations by parts lead to

$$\begin{aligned} T_{k_1}(\eta) &= - (k_2^3 + k_3^3) \int^\eta \frac{d\eta_1}{\eta_1} e^{-i(c_s k_1 + k_2 + k_3)\eta_1} \\ &+ \left(\frac{i}{\eta^3} - \frac{c_s k_1 + k_2 + k_3}{\eta^2} - i \frac{c_s k_1 (k_2 + k_3) - k_2^2 + k_2 k_3 - k_3^2}{\eta} + \frac{c_s^2 k_1^2 k_2 k_3}{c_s k_1 + k_2 + k_3} \right) e^{-i(c_s k_1 + k_2 + k_3)\eta}, \end{aligned}$$

and

$$\begin{aligned} H_{k_3}(\eta) &= -3k_3^3 \int^\eta \frac{d\eta_1}{\eta_1} e^{-i(c_s k_1 + c_s k_2 + k_3)\eta_1} + i \frac{c_s^4 k_1^2 k_2^2 k_3}{c_s k_1 + c_s k_2 + k_3} \eta e^{-i(c_s k_1 + c_s k_2 + k_3)\eta} \\ &+ \frac{c_s^3 k_1 k_2 (c_s^2 k_1 k_2 (k_1 + k_2) + c_s k_3 (3k_1^2 + 8k_1 k_2 + 3k_2^2) + 3(k_1 + k_2) k_3^2)}{(c_s k_1 + c_s k_2 + k_3)^2} e^{-i(c_s k_1 + c_s k_2 + k_3)\eta} \\ &+ \left(\frac{3i}{\eta^3} - \frac{3(c_s k_1 + c_s k_2 + k_3)}{\eta^2} - i \frac{3(c_s^2 k_1 k_2 + c_s k_3 (k_1 + k_2) - k_3^2)}{\eta} \right) e^{-i(c_s k_1 + c_s k_2 + k_3)\eta}. \end{aligned}$$

All the terms with negative powers of η cancel when taking the imaginary parts, due to the rapid decay of the imaginary part of the propagators beyond the Hubble horizon;

$$\Im(g_k^*(\eta)u_k(\eta)) = k^3\eta^3 + O(\eta^5) \quad \text{and} \quad \Im(h_k^*(\eta)v_k(\eta)) = c_s^3 k^3 \eta^3 + O(\eta^5).$$

The end results are again logarithmic dependences on η ;

$$\begin{aligned} \langle \xi_{k_1} \xi_{k_2} \alpha'_{k_3} \rangle &\rightarrow -\frac{27H^3 \mathcal{I}(k_1^3 + k_2^3)}{\sqrt{\epsilon_\varphi} \eta^6 c_s^3 k_1^3 k_2^3 k_3^3} \int^\eta \frac{d\eta_1}{\eta_1} \cos[(k_1 + k_2 + c_s k_3)(\eta - \eta_1)], \\ \langle \xi_{k_1} \alpha'_{k_2} \alpha'_{k_3} \rangle &\rightarrow \frac{27H^2 k_1^3}{2\sqrt{2\epsilon_\varphi} \eta^9 c_s^6 k_1^3 k_2^3 k_3^3} \int^\eta \frac{d\eta_1}{\eta_1} \cos[(k_1 + c_s k_2 + c_s k_3)(\eta - \eta_1)]. \end{aligned}$$

A.2 2-vertex contributions

Let us start from the term (3.9). By definition, the connected tree-level contribution is given by

$$\begin{aligned} -\langle H^B(\eta_2) H^q(\eta_1) \xi^3 \rangle &= \frac{12\mathcal{I}}{\sqrt{\epsilon_\varphi} H} \int d^3 w_2 \frac{6\sqrt{2}\mathcal{I}}{H} \int d^3 w_1 \langle \pi(\mathbf{w}_2)^2 \alpha'(\mathbf{w}_2) \pi(\mathbf{w}_1) \alpha'(\mathbf{w}_1) \xi(\mathbf{x}) \xi(\mathbf{y}) \xi(\mathbf{z}) \rangle \\ &= \sqrt{\frac{2}{\epsilon_\varphi}} \frac{144\mathcal{I}^2}{H^2} \iint d^3 w_2 d^3 w_1 \langle \alpha'(\mathbf{w}_2) \alpha'(\mathbf{w}_1) \rangle (\langle \pi(\mathbf{w}_2) \xi(\mathbf{y}) \rangle \langle \pi(\mathbf{w}_2) \xi(\mathbf{z}) \rangle \langle \pi(\mathbf{w}_1) \xi(\mathbf{x}) \rangle + 2 \text{ perms}). \end{aligned}$$

Given

$$\begin{aligned} \langle \pi(\eta_1, \mathbf{w}_1) \xi(\eta, \mathbf{x}) \rangle &= \int \frac{d^3 k_1}{(2\pi)^3} \frac{H^2}{2k_1^3 \eta} u_{k_1}(\eta_1) g_{k_1}^*(\eta) e^{-i\mathbf{k}_1 \cdot (\mathbf{x} - \mathbf{w}_1)}, \\ \langle \alpha'(\eta_2, \mathbf{w}_2) \alpha'(\eta_1, \mathbf{w}_1) \rangle &= \int \frac{d^3 p}{(2\pi)^3} \frac{1}{6c_s^3 p^3 \eta_1^4 \eta_2^4} h_p(\eta_2) h_p^*(\eta_1) e^{-i\mathbf{p} \cdot (\mathbf{w}_1 - \mathbf{w}_2)}, \end{aligned}$$

we can write down its Fourier transform as

$$\begin{aligned} -\langle H^B(\eta_2) H^q(\eta_1) \xi_k^3 \rangle &= \sqrt{\frac{2}{\epsilon_\varphi}} \frac{3H^4 \mathcal{I}^2}{c_s^3 k_1^6 k_2^3 k_3^3 \eta^3} g_{k_1}^*(\eta) g_{k_2}^*(\eta) g_{k_3}^*(\eta) u_{k_1}(\eta_1) \frac{h_{k_1}^*(\eta_1)}{\eta_1^4} u_{k_2}(\eta_2) u_{k_3}(\eta_2) \frac{h_{k_1}(\eta_2)}{\eta_2^4} \\ &\quad + 2 \text{ perms.} \end{aligned}$$

Taking the commutators, it becomes

$$\begin{aligned} -\langle [H^B(\eta_2), [H^q(\eta_1), \xi_k^3]] \rangle &= -\sqrt{\frac{2}{\epsilon_\varphi}} \frac{12H^4 \mathcal{I}^2}{c_s^3 k_1^6 k_2^3 k_3^3 \eta^3} \Im(g_{k_1}^*(\eta) u_{k_1}(\eta_1)) \\ &\quad \times \Im\left(g_{k_2}^*(\eta) g_{k_3}^*(\eta) \frac{h_{k_1}^*(\eta_1)}{\eta_1^4} u_{k_2}(\eta_2) u_{k_3}(\eta_2) \frac{h_{k_1}(\eta_2)}{\eta_2^4}\right) + 2 \text{ perms.} \end{aligned}$$

Now our task is to carry out the integral

$$\mathcal{A}_{2a} = \int^\eta \frac{d\eta_1}{\eta_1^4} \Im(g_{k_1}^* u_{k_1}(\eta_1)) \Im(g_{k_2}^* g_{k_3}^* h_{k_1}^*(\eta_1) T_{k_1}(\eta_1)).$$

Substituting the integrated expression for $T_{k_1}(\eta_1)$, the single integral arising from its second line gives at most $\propto \ln(-\eta)$ in the limit $\eta \rightarrow 0$ since any power divergence disappears after

taking the imaginary part as demonstrated for the 1-vertex cases.² We then only have to check if the remaining term gives rise to similar logarithmic contributions. Evaluating the double integral, we obtain

$$\begin{aligned}
& \int^\eta \frac{d\eta_1}{\eta_1^4} \Im(g_{k_1}^* u_{k_1}(\eta_1)) \Im\left(g_{k_2}^* g_{k_3}^* h_{k_1}^*(\eta_1) \int^{\eta_1} \frac{d\eta_2}{\eta_2} e^{-i(c_s k_1 + k_2 + k_3)\eta_2}\right) \\
&= -k_1^3 \int^\eta \frac{d\eta_1}{\eta_1} \Im(g_{k_1}^* e^{-ik_1 \eta_1}) \Im\left(g_{k_2}^* g_{k_3}^* v_{k_1}^*(\eta_1) \int^{\eta_1} \frac{d\eta_2}{\eta_2} e^{-i(c_s k_1 + k_2 + k_3)\eta_2}\right) \\
&+ \frac{1}{\eta^3} \Im(g_{k_1}^* [u_{k_1} + ik_1^2 \eta^2 e^{-ik_1 \eta}]) \Im\left(g_{k_2}^* g_{k_3}^* v_{k_1}^* \int^\eta \frac{d\eta_1}{\eta_1} e^{-i(c_s k_1 + k_2 + k_3)\eta_1}\right) \\
&- c_s^2 k_1^4 \int^\eta d\eta_1 \Im(i g_{k_1}^* e^{-ik_1 \eta_1}) \Im\left(i g_{k_2}^* g_{k_3}^* e^{ic_s k_1 \eta_1} \int^{\eta_1} \frac{d\eta_2}{\eta_2} e^{-i(c_s k_1 + k_2 + k_3)\eta_2}\right) \\
&- \int^\eta \frac{d\eta_1}{\eta_1^4} \Im(g_{k_1}^* [u_{k_1}(\eta_1) + ik_1^2 \eta_1^2 e^{-ik_1 \eta_1}]) \Im(g_{k_2}^* g_{k_3}^* v_{k_1}^*(\eta_1) e^{-i(c_s k_1 + k_2 + k_3)\eta_1}).
\end{aligned}$$

All the integrations are at most of order $\ln(-\eta)$ as $\eta \rightarrow 0$ except for the first line whose leading term yields

$$\mathcal{A}_{2a} \rightarrow 27k_1^3(k_2^3 + k_3^3) \int^\eta \frac{d\eta_1}{\eta_1} \int^{\eta_1} \frac{d\eta_2}{\eta_2} \cos(k_1(\eta - \eta_1)) \cos(c_s k_1(\eta_1 - \eta_2) + (k_2 + k_3)(\eta - \eta_2))$$

and behaves as $(\ln(-\eta))^2$. The leading-order behaviors for the other contributions are essentially the same. For (3.10), the amplitude reads

$$\begin{aligned}
-\langle [H^q(\eta_2), [H^B(\eta_1), \xi_k^3]] \rangle &= -\sqrt{\frac{2}{\epsilon_\varphi}} \frac{12H^4 \mathcal{I}^2}{c_s^3 k_1^6 k_2^3 k_3^3 \eta^3} \Im(g_{k_2}^*(\eta) g_{k_3}^*(\eta) u_{k_2}(\eta_1) u_{k_3}(\eta_1)) \\
&\times \Im\left(g_{k_1}^*(\eta) \frac{h_{k_1}^*(\eta_1)}{\eta_1^4} u_{k_1}(\eta_2) \frac{h_{k_1}(\eta_2)}{\eta_2^4}\right) + 2 \text{ perms.}
\end{aligned}$$

Defining

$$\begin{aligned}
F_{k_1}(\eta_1) &= \int^{\eta_1} \frac{d\eta_2}{\eta_2^4} u_{k_1}(\eta_2) h_{k_1}(\eta_2) \\
&= \frac{1}{\eta_1^3} u_{k_1}(\eta_1) v_{k_1}(\eta_1) + \frac{k_1^2}{\eta_1} e^{-ik_1(1+c_s)\eta_1} + ik_1^3 \int^{\eta_1} \frac{d\eta_2}{\eta_2} e^{-ik_1(1+c_s)\eta_2},
\end{aligned}$$

we retain only the most divergent term to obtain

$$\begin{aligned}
\mathcal{A}_{2b} &= \int^\eta \frac{d\eta_1}{\eta_1^4} \Im(g_{k_2}^* g_{k_3}^* u_{k_2}(\eta_1) u_{k_3}(\eta_1)) \Im(g_{k_1}^* h_{k_1}^*(\eta_1) F_{k_1}(\eta_1)) \\
&\sim -k_1^3 \int^\eta \frac{d\eta_1}{\eta_1} \Im(g_{k_2}^* g_{k_3}^* [k_2^3 e^{-ik_2 \eta_1} u_{k_3} + k_3^3 e^{-ik_3 \eta_1} u_{k_2}]) \Im\left(i g_{k_1}^* v_{k_1}^* \int^{\tau_1} \frac{d\eta_2}{\eta_2} e^{-ik_1(1+c_s)\eta_2}\right) \\
&\sim 27k_1^3(k_2^3 + k_3^3) \int^\eta \frac{d\eta_1}{\eta_1} \int^{\eta_1} \frac{d\eta_2}{\eta_2} \cos((k_1 + k_2)(\eta - \eta_1)) \cos(k_1(\eta - \eta_2) + c_s k_1(\eta_1 - \eta_2)).
\end{aligned}$$

²In fact, one can directly show there is no power divergence by Taylor-expanding the propagators (A.1) and (A.2). Namely, the integrand does not contain any power of η , η_1 and η_2 lower than -1 when the exponential is written as a power series. Since the calculation relies on Mathematica, however, we stick to the integrations by parts here.

For (3.15),

$$-\langle H^C(\eta_2)H^q(\eta_1)\xi(\mathbf{x})\xi(\mathbf{y})\alpha'(\mathbf{z})\rangle = -\frac{72\mathcal{I}}{\sqrt{\epsilon_\varphi}H}\tau_2^4 \iint d^3w_1 d^3w_2 \langle \alpha'(\mathbf{w}_2)\alpha'(\mathbf{w}_1)\rangle \langle \alpha'(\mathbf{w}_2)\alpha'(\mathbf{z})\rangle \\ \times (\langle \pi(\mathbf{w}_2)\xi(\mathbf{y})\rangle \langle \pi(\mathbf{w}_1)\xi(\mathbf{x})\rangle \langle \pi(\mathbf{w}_2)\xi(\mathbf{x})\rangle \langle \pi(\mathbf{w}_1)\xi(\mathbf{y})\rangle),$$

and in Fourier space, it becomes

$$-\langle H^C(\eta_2)H^q(\eta_1)\xi_{k_1}\xi_{k_2}\alpha'_{k_3}\rangle = -\frac{H^3\mathcal{I}}{2\sqrt{\epsilon_\varphi}\eta^6 c_s^6 k_1^6 k_2^3 k_3^3} g_{k_1}^*(\eta)g_{k_2}^*(\eta)h_{k_3}^*(\eta) \\ \times u_{k_1}(\eta_1)\frac{h_{k_1}^*(\eta_1)}{\eta_1^4}h_{k_1}(\eta_2)u_{k_2}(\eta_2)\frac{h_{k_3}(\eta_2)}{\eta_2^4} + (1 \leftrightarrow 2).$$

Then, we derive

$$-[\langle H^C(\eta_2), [H^q(\eta_1), \xi_{k_1}\xi_{k_2}\alpha'_{k_3}] \rangle] = \frac{2H^3\mathcal{I}}{\sqrt{\epsilon_\varphi}c_s^6 k_1^6 k_2^3 k_3^3 \eta^6} \Im(g_{k_1}^*(\eta)u_{k_1}(\eta_1)) \\ \times \Im\left(g_{k_2}^*(\eta)h_{k_3}^*(\eta)\frac{h_{k_1}^*(\eta_1)}{\eta_1^4}h_{k_1}(\eta_2)u_{k_2}(\eta_2)\frac{h_{k_3}(\eta_2)}{\eta_2^4}\right) + (1 \leftrightarrow 2).$$

As before, integration goes as

$$\mathcal{B}_{2a} = \int^\eta \frac{d\eta_1}{\eta_1^4} \Im(g_{k_1}^* u_{k_1}(\eta_1)) \Im(g_{k_2}^* h_{k_3}^* h_{k_1}^*(\eta_1) H_{k_2}(\eta_1)) \\ \sim -3k_2^3 \int^\eta \frac{d\eta_1}{\eta_1^4} \Im(g_{k_1}^* u_{k_1}) \Im\left(g_{k_2}^* h_{k_3}^* h_{k_1}^* \int^{\eta_1} \frac{d\eta_2}{\eta_2} e^{-i(c_s k_1 + k_2 + c_s k_3)\eta_2}\right) \\ \sim 3k_1^3 k_2^3 \int^\eta \frac{d\eta_1}{\eta_1} \Im(g_{k_1}^* u^{-ik_1 \eta_1}) \Im\left(g_{k_2}^* h_{k_3}^* v_{k_1}^*(\eta_1) \int^{\eta_1} \frac{d\eta_2}{\eta_2} e^{-i(c_s k_1 + k_2 + c_s k_3)\eta_2}\right) \\ \sim 81k_1^3 k_2^3 \int^\eta \frac{d\eta_1}{\eta_1} \int^{\eta_1} \frac{d\eta_2}{\eta_2} \cos(k_1(\eta - \eta_1)) \cos(c_s k_1(\eta_1 - \eta_2) + (k_2 + c_s k_3)(\eta - \eta_2)).$$

Finally, (3.16) yields

$$-\langle [H^q(\eta_2), [H^C(\eta_1), \xi_{k_1}\xi_{k_2}\alpha'_{k_3}]] \rangle = \frac{2H^3\mathcal{I}}{\sqrt{\epsilon_\varphi}c_s^6 k_1^6 k_2^3 k_3^3 \eta^6} \Im\left(g_{k_2}^*(\eta)h_{k_3}^*(\eta)u_{k_2}(\eta_1)\frac{h_{k_3}(\eta_1)}{\tau_1^4}\right) \\ \times \Im\left(g_{k_1}^*(\eta)h_{k_1}^*(\eta_1)\frac{h_{k_1}(\eta_2)}{\eta_2^4}u_{k_1}(\eta_2)\right) + (1 \leftrightarrow 2).$$

The leading-order contribution is

$$\mathcal{B}_{2b} = \int^\eta \frac{d\eta_1}{\eta_1^4} \Im(g_{k_2}^* h_{k_3}^* u_{k_2}(\eta_1)h_{k_3}(\eta_1)) \Im(g_{k_1}^* h_{k_1}^*(\eta_1)F_{k_1}(\eta_1)) \\ \sim -k_1^3 k_2^3 \int^\eta \frac{d\eta_1}{\eta_1} \Im(g_{k_2}^* h_{k_3}^* e^{-ik_2 \eta_1} h_{k_3}(\eta_1)) \Im\left(ig_{k_1}^* v_{k_1}^*(\eta_1) \int^{\eta_1} \frac{d\eta_2}{\eta_2} e^{-i(1+c_s)k_1 \eta_2}\right) \\ \sim 81k_1^3 k_2^3 \int^\eta \frac{d\eta_1}{\eta_1} \int^{\eta_1} \frac{d\eta_2}{\eta_2} \cos((k_2 + c_s k_3)(\eta - \eta_1)) \cos(c_s k_1(\eta_1 - \eta_2) + k_1(\eta - \eta_2)).$$

A.3 3-vertex contributions

We saw that the 1-vertex terms that involve only single time integrals resulted in $\propto \ln(-\eta)$ while the leading contributions from 2-vertex terms come from double integrals and proportional to $(\ln(-\eta))^2$. Hence, one expects that 3-vertex contributions behave like $(\ln(-\eta))^3$ and dominate the tree-level amplitude at the order \mathcal{I}^2 . This was also the result of [55]. We explicitly prove it and derive the coefficients in front. The principle of the calculations is the same as the previous sections although the algebra gets increasingly complicated. First of all, we write

$$\begin{aligned} -i\langle H^C(\eta_3)H^q(\eta_2)H^q(\eta_1)\xi(\mathbf{x})\xi(\mathbf{y})\xi(\mathbf{z})\rangle &= -i3\eta_3^4\sqrt{\frac{2}{\epsilon_\varphi}}\frac{144\mathcal{I}^2}{H^2}\iiint d^3w_1^3d^3w_2^3d^3w_3 \\ &\times\langle\alpha'(\mathbf{w}_3)\alpha'(\mathbf{w}_2)\rangle\langle\alpha'(\mathbf{w}_3)\alpha'(\mathbf{w}_1)\rangle(\langle\pi(\mathbf{w}_3)\xi(\mathbf{z})\rangle\langle\pi(\mathbf{w}_2)\xi(\mathbf{y})\rangle\langle\pi(\mathbf{w}_1)\xi(\mathbf{x})\rangle+5\text{ perms}) \end{aligned}$$

and

$$\begin{aligned} \langle H^C(\eta_3)H^q(\eta_2)H^q(\eta_1)\xi_{k_1}\xi_{k_2}\xi_{k_3}\rangle &= \frac{3H^4\mathcal{I}^2}{\sqrt{2\epsilon_\varphi}\eta^3(\eta_1\eta_2\eta_3)^4}\frac{1}{c_s^6k_1^6k_2^6k_3^3}g_{k_1}^*(\eta)g_{k_2}^*(\eta)g_{k_3}^*(\eta) \\ &\times u_{k_1}(\eta_1)h_{k_1}^*(\eta_1)u_{k_2}(\eta_2)h_{k_2}^*(\eta_2)h_{k_1}(\eta_3)h_{k_2}(\eta_3)u_{k_3}(\eta_3)+5\text{ perms.} \end{aligned}$$

In the end, our integrand is

$$\begin{aligned} -i\langle[H^C(\eta_3),[H^q(\eta_2),[H^q(\eta_1),\xi_k^3]]]\rangle &= -\sqrt{\frac{2}{\epsilon_\varphi}}\frac{12H^4\mathcal{I}^2}{\eta^3(\eta_1\eta_2\eta_3)^4}\frac{1}{c_s^6k_1^6k_2^6k_3^3} \\ &\times\Im(g_{k_1}^*u_{k_1}(\eta_1))\Im(g_{k_2}^*u_{k_2}(\eta_2))\Im(g_{k_3}^*h_{k_1}^*(\eta_1)h_{k_2}^*(\eta_2)h_{k_1}(\eta_3)h_{k_2}(\eta_3)u_{k_3}(\eta_3))+5\text{ perms.} \end{aligned}$$

Anticipating the cancellation of terms with negative powers of η , we seek the expected $(\ln(-\eta))^3$ contribution. It can only come from

$$\begin{aligned} \mathcal{A}_{3a} &= \int^\eta \frac{d\eta_1}{\eta_1^4}\Im(g_{k_1}^*u_{k_1}(\eta_1))\int^{\eta_1}\frac{d\eta_2}{\eta_2^4}\Im(g_{k_2}^*u_{k_2}(\eta_2))\Im(g_{k_3}^*h_{k_1}^*(\eta_1)h_{k_2}^*(\eta_2)H_{k_3}(\eta_2)) \\ &\sim 3k_2^3k_3^3\int^\eta \frac{d\eta_1}{\eta_1^4}\Im(g_{k_1}^*u_{k_1}(\eta_1))\int^{\eta_1}\frac{d\eta_2}{\eta_2}\Im(g_{k_2}^*e^{-ik_2\eta_2}) \\ &\quad \times\Im\left(g_{k_3}^*h_{k_1}^*(\eta_1)v_{k_2}^*(\eta_2)\int^{\eta_2}\frac{d\eta_3}{\eta_3}e^{-i(c_sk_1+c_sk_2+k_3)\eta_3}\right) \end{aligned}$$

where we integrated by parts for η_2 . We perform another integration by parts with η_1 as follows:

$$\begin{aligned} &\int^\eta d\eta_1\Im(g_{k_1}^*u_{k_1}(\eta_1))\int^{\eta_1}\frac{d\eta_2}{\eta_2}\Im(g_{k_2}^*e^{-ik_2\eta_2})\Im\left(g_{k_3}^*\left(\frac{v_{k_1}^*(\eta_1)}{\eta_1^3}\right)'v_{k_2}^*(\eta_2)\int^{\eta_2}\frac{d\eta_3}{\eta_3}e^{-i(c_sk_1+c_sk_2+k_3)\eta_3}\right) \\ &= \frac{1}{\eta^3}\Im(g_{k_1}^*u_{k_1})\int^\eta \frac{d\eta_2}{\eta_2}\Im(g_{k_2}^*e^{-ik_2\eta_2})\Im\left(g_{k_3}^*v_{k_1}^*(\eta)v_{k_2}^*(\eta_2)\int^{\eta_2}\frac{d\eta_3}{\eta_3}e^{-i(c_sk_1+c_sk_2+k_3)\eta_3}\right) \\ &\quad - \int^\eta \frac{d\eta_1}{\eta_1^2}\Im(ik_1^2g_{k_1}e^{-ik_1\eta_1})\int^{\eta_1}\frac{d\eta_2}{\eta_2}\Im(g_{k_2}^*e^{-ik_2\eta_2})\Im\left(g_{k_3}^*v_{k_1}^*(\eta_1)v_{k_2}^*(\eta_2)\int^{\eta_2}\frac{d\eta_3}{\eta_3}e^{-i(c_sk_1+c_sk_2+k_3)\eta_3}\right) \\ &\quad - \int^\eta \frac{d\eta_1}{\eta_1^4}\Im(g_{k_1}^*u_{k_1}(\eta_1))\Im(g_{k_1}^*e^{-ik_2\eta_1})\Im\left(g_{k_3}^*v_{k_1}^*(\eta_1)v_{k_2}^*(\eta_1)\int^{\eta_1}\frac{d\eta_3}{\eta_3}e^{-i(c_sk_1+c_sk_2+k_3)\eta_3}\right). \end{aligned}$$

Only the second term can give rise to the sought dependence on η . We derive

$$\begin{aligned}\mathcal{A}_{3a} &\sim -3k_1^3 k_2^3 k_3^3 \int^\eta \frac{d\eta_1}{\eta_1} \Im \left(g_{k_1}^* e^{-ik_1 \eta_1} \right) \int^{\eta_1} \frac{d\eta_2}{\eta_2} \Im \left(g_{k_2}^* e^{-ik_2 \eta_2} \right) \\ &\quad \times \Im \left(g_{k_3}^* v_{k_1}^*(\eta_1) v_{k_2}^*(\eta_2) \int^{\eta_2} \frac{d\eta_3}{\eta_3} e^{-i(c_s k_1 + c_s k_2 + k_3) \eta_3} \right) \\ &\sim -81k_1^3 k_2^3 k_3^3 \int^\eta \frac{d\eta_1}{\eta_1} \cos(k_1(\eta - \eta_1)) \int^{\eta_1} \frac{d\eta_2}{\eta_2} \cos(k_2(\eta - \eta_2)) \\ &\quad \times \int^{\eta_2} \frac{d\eta_3}{\eta_3} \cos(c_s k_1(\eta_1 - \eta_3) + c_s k_2(\eta_2 - \eta_3) + k_3(\eta - \eta_3)).\end{aligned}$$

For (3.12), we have

$$\begin{aligned}-i\langle H^q(\eta_3) H^C(\eta_2) H^q(\eta_1) \xi(\mathbf{x}) \xi(\mathbf{y}) \xi(\mathbf{z}) \rangle &= -i3\eta_2^4 \sqrt{\frac{2}{\epsilon_\varphi} \frac{144\mathcal{I}^2}{H^2}} \iiint d^3 w_1 d^3 w_2 d^3 w_3 \\ &\times \langle \alpha'(\mathbf{w}_3) \alpha'(\mathbf{w}_2) \rangle \langle \alpha'(\mathbf{w}_2) \alpha'(\mathbf{w}_1) \rangle (\langle \pi(\mathbf{w}_3) \xi(\mathbf{z}) \rangle \langle \pi(\mathbf{w}_2) \xi(\mathbf{y}) \rangle \langle \pi(\mathbf{w}_1) \xi(\mathbf{x}) \rangle + 5 \text{ perms}),\end{aligned}$$

and

$$\begin{aligned}-i\langle [H^q(\eta_3), [H^C(\eta_2), [H^q(\eta_1), \xi_k^3]]] \rangle &= -\sqrt{\frac{2}{\epsilon_\varphi} \frac{12H^4\mathcal{I}^2}{\eta^3(\eta_1\eta_2\eta_3)^4}} \frac{1}{c_s^6 k_1^6 k_2^3 k_3^6} \\ &\times \Im(g_{k_1}^* u_{k_1}(\eta_1)) \Im(g_{k_2}^* h_{k_1}^*(\eta_1) u_{k_2}(\eta_2) h_{k_1}(\eta_2)) \Im(g_{k_3}^* h_{k_3}^*(\eta_2) u_{k_3}(\eta_3) h_{k_3}(\eta_3)) + 5 \text{ perms}.\end{aligned}$$

The integration results in

$$\begin{aligned}\mathcal{A}_{3b} &= \int^\eta \frac{d\eta_1}{\eta_1^4} \Im(g_{k_1}^* u_{k_1}(\eta_1)) \int^{\eta_1} \frac{d\eta_2}{\eta_2^4} \Im(g_{k_2}^* h_{k_1}^*(\eta_1) u_{k_2}(\eta_2) h_{k_1}(\eta_2)) \Im(g_{k_3}^* h_{k_3}^*(\eta_2) F_{k_3}(\eta_2)) \\ &\sim k_1^3 k_2^3 k_3^3 \int^\eta \frac{d\eta_1}{\eta_1} \Im(g_{k_1}^* e^{-ik_1 \eta_1}) \int^{\eta_1} \frac{d\eta_2}{\eta_2} \Im(g_{k_2}^* v_{k_1}^*(\eta_1) e^{-ik_2 \eta_2} h_{k_1}(\eta_2)) \\ &\quad \times \Im\left(ig_{k_3}^* v_{k_3}^*(\eta_2) \int^{\eta_2} \frac{d\eta_3}{\eta_3} e^{-i(1+c_s)k_3 \eta_3}\right) \\ &\sim -81k_1^3 k_2^3 k_3^3 \int^\eta \frac{d\eta_1}{\eta_1} \cos(k_1(\eta - \eta_1)) \int^{\eta_1} \frac{d\eta_2}{\eta_2} \cos(c_s k_1(\eta_1 - \eta_2) + k_2(\eta - \eta_2)) \\ &\quad \times \int^{\eta_2} \frac{d\eta_3}{\eta_3} \cos(k_3(\eta - \eta_3) + c_s k_3(\eta_2 - \eta_3)).\end{aligned}$$

For (3.13), we have

$$\begin{aligned}-i\langle H^q(\eta_3) H^q(\eta_2) H^C(\eta_1) \xi(\mathbf{x}) \xi(\mathbf{y}) \xi(\mathbf{z}) \rangle &= -i3\eta_2^4 \sqrt{\frac{2}{\epsilon_\varphi} \frac{144\mathcal{I}^2}{H^2}} \iiint d^3 w_1 d^3 w_2 d^3 w_3 \\ &\times \langle \alpha'(\mathbf{w}_3) \alpha'(\mathbf{w}_1) \rangle \langle \alpha'(\mathbf{w}_2) \alpha'(\mathbf{w}_1) \rangle (\langle \pi(\mathbf{w}_3) \xi(\mathbf{z}) \rangle \langle \pi(\mathbf{w}_2) \xi(\mathbf{y}) \rangle \langle \pi(\mathbf{w}_1) \xi(\mathbf{x}) \rangle + 5 \text{ perms}),\end{aligned}$$

and

$$\begin{aligned}-i\langle [H^q(\eta_3), [H^q(\eta_2), [H^C(\eta_1), \xi_k^3]]] \rangle &= -\sqrt{\frac{2}{\epsilon_\varphi} \frac{12H^4\mathcal{I}^2}{\eta^3(\eta_1\eta_2\eta_3)^4}} \frac{1}{c_s^6 k_1^6 k_2^3 k_3^6} \\ &\times \Im(g_{k_1}^* u_{k_1}(\eta_1)) \Im(g_{k_2}^* h_{k_1}^*(\eta_1) u_{k_2}(\eta_2) h_{k_1}(\eta_2)) \Im(g_{k_3}^* h_{k_3}^*(\eta_1) u_{k_3}(\eta_3) h_{k_3}(\eta_3)) + 5 \text{ perms}.\end{aligned}$$

Similar to the other two, we obtain

$$\begin{aligned}
\mathcal{A}_{3c} &= \int^\eta \frac{d\eta_1}{\eta_1^4} \Im(g_{k_1}^* u_{k_1}(\eta_1)) \int^{\eta_1} \frac{d\eta_2}{\eta_2^4} \Im(g_{k_2}^* h_{k_1}^*(\eta_1) u_{k_2}(\eta_2) h_{k_1}(\eta_2)) \Im(g_{k_3}^* h_{k_3}^*(\eta_1) F_{k_3}(\eta_2)) \\
&\sim -k_2^3 k_3^3 \int^\eta \frac{d\eta_1}{\eta_1^4} \Im(g_{k_1}^* u_{k_1}(\eta_1)) \int^{\eta_1} \frac{d\eta_2}{\eta_2^2} \Im(g_{k_2}^* h_{k_1}^*(\eta_1) e^{-ik_2 \eta_2} v_{k_1}(\eta_2)) \\
&\quad \times \Im\left(ig_{k_3}^* h_{k_3}^*(\eta_1) \int^{\eta_2} \frac{d\eta_3}{\eta_3} e^{-i(1+c_s)k_3 \eta_3}\right) \\
&\sim k_2^3 k_3^3 \int^\eta \frac{d\eta_1}{\eta_1^2} \Im(ik_1^2 g_{k_1}^* e^{-ik_1 \eta_1}) \int^{\eta_1} \frac{d\eta_2}{\eta_2} \Im(g_{k_2}^* v_{k_1}^*(\eta_1) e^{-ik_2 \eta_2} v_{k_1}(\eta_2)) \\
&\quad \times \Im\left(ig_{k_3}^* h_{k_3}^*(\eta_1) \int^{\eta_2} \frac{d\eta_3}{\eta_3} e^{-i(1+c_s)k_3 \eta_3}\right) \\
&\sim k_1^3 k_2^3 k_3^3 \int^\eta \frac{d\eta_1}{\eta_1} \Im(g_{k_1}^* e^{-ik_1 \eta_1}) \int^{\eta_1} \frac{d\eta_2}{\eta_2} \Im(g_{k_2}^* v_{k_1}^*(\eta_1) e^{-ik_2 \eta_2} v_{k_1}(\eta_2)) \\
&\quad \times \Im\left(ig_{k_3}^* h_{k_3}^*(\eta_1) \int^{\eta_2} \frac{d\eta_3}{\eta_3} e^{-i(1+c_s)k_3 \eta_3}\right) \\
&\sim -81k_1^3 k_2^3 k_3^3 \int^\eta \frac{d\eta_1}{\eta_1} \cos(k_1(\eta - \eta_1)) \int^{\eta_1} \frac{d\eta_2}{\eta_2} \cos(c_s k_1(\eta_1 - \eta_2) + k_2(\eta - \eta_2)) \\
&\quad \times \int^{\eta_2} \frac{d\eta_3}{\eta_3} \cos(k_3(\eta - \eta_3) + c_s k_3(\eta_1 - \eta_3)).
\end{aligned}$$

A.4 Second order curvature perturbation and summary

So far, we have only discussed the linear part of the curvature perturbation since it is the only term that picks up contributions from cubic vertices at tree level. The second- and higher order terms in ζ also contribute to the bispectrum, however, through the combinations such as $\langle \zeta_{(1)} \zeta_{(1)} \zeta_{(2)} \rangle$. Since it is impossible to examine at all orders if they give any contribution within the order \mathcal{I}^2 , here we just look at the second-order term and check that they do not become dominant over the 3-vertex contributions derived in the previous subsection.

First, we note that ignoring higher order corrections in $\epsilon_{H,\varphi}, \eta_{H,\varphi}$ and the terms with spatial derivatives and using (2.17), we can rewrite Ξ_{ij} as

$$\Xi_{ij} = \left(4\zeta_{(1)}^2 - \frac{2}{\bar{\rho}'} \delta \rho'_{(1)} \zeta_{(1)}\right) \delta_{ij} - \frac{2}{\mathcal{H}} \left(\zeta_{(1),i} B_{,j}^{(1)} + \zeta_{(1),j} B_{,i}^{(1)}\right).$$

Comparing equation (3.3) with

$$\nabla^2 B^{(1)} = -\sqrt{\frac{\epsilon_\varphi}{2}} \left[\pi' + \frac{6\mathcal{I}}{\eta} \pi - \frac{3}{\sqrt{2}} H \eta^3 \left(\alpha' - \frac{2}{\eta} \alpha\right)\right],$$

we see the second term is suppressed by a factor of ϵ_H . Throwing it away, equation (2.18) yields

$$-\zeta_{(2)} = \frac{\mathcal{H}}{\bar{\rho}'} \delta \rho_{(2)} + 2 \frac{\delta \rho'_{(1)}}{\bar{\rho}'} \zeta_{(1)} - 2\zeta_{(1)}^2.$$

Expanding the energy-momentum tensor up to second order, we find

$$\begin{aligned}\delta\rho_{(2)} &= -2T_{(2)0}^0 + \frac{2}{\bar{\rho} + \bar{p}} T_{(1)i}^0 T_{(1)0}^i \\ &= \frac{1}{a^2} \pi'^2 + \frac{1}{a^2} \pi_{,i} \pi_{,i} + \left(V_{,\varphi\varphi} + \frac{3c^2}{a^2 f^2} \frac{(f^2)_{,\varphi\varphi}}{f^2} \frac{1}{a^2} \right) \pi^2 + \frac{1}{a^2} \left(\bar{\varphi}'^2 + \frac{3c^2}{a^2 f^2} \right) (3\phi_{(1)}^2 - \phi_{(2)}) \\ &\quad - \frac{4\bar{\varphi}'}{a^2} \phi_{(1)} \pi' - \frac{2c^2}{a^2 f^2} \frac{(f^2)_{,\varphi}}{f^2} \frac{1}{a^2} \phi_{(1)} \pi + \frac{6c}{af} \frac{(f^2)_{,\varphi}}{f^2} \frac{f}{a^3} \pi \alpha' - \frac{12c}{af} \frac{f}{a^3} \phi_{(1)} \alpha' + \frac{f^2}{a^4} (3\alpha'^2 + 2\alpha_{,i} \alpha_{,i}).\end{aligned}$$

The appearance of $\phi_{(2)}$ forces us to look into the constraint equations at the second order. In fact, they are not too bad for the scalar perturbations in the flat gauge. The relevant equation is obtained from variation of N_i in the ADM formalism and reads

$$-\frac{2\mathcal{H}\delta_{ij} + B_{,ij} - \nabla^2 B \delta_{ij}}{1 + \phi} \phi_{,i} = -\varphi' \varphi_{,j} + \varphi_{,i} B_{,i} \varphi_{,j} + f^2 L_i^a F_{,j}^{ai}.$$

Expanding it to the second order, we find

$$\begin{aligned}2\mathcal{H}\phi_{(2),j} &= \left(2\mathcal{H}\phi_{(1)} + \nabla^2 B^{(1)} \right) \phi_{(1),j} - B_{,ij}^{(1)} \phi_{(1),i} \\ &\quad + \pi' \pi_{,j} + \frac{f^2}{a^2} (2\alpha' \alpha_{,j} + \tau'_{,i} \tau_{,ij} + \tau'_{,j} \nabla^2 \tau).\end{aligned}\tag{A.4}$$

In the end, its contribution is subdominant. Keeping the leading-order terms in slow roll and discarding higher spatial derivatives, we obtain

$$\zeta_{(2)} = \frac{\eta^2}{6\epsilon_H} \pi'^2 + \frac{1}{6\epsilon_H} (24\mathcal{I}^2 \pi^2 - 12H\mathcal{I} \eta^4 \pi \alpha' + 3H^2 \eta^8 \alpha'^2) + 2\zeta_{(1)}^2 - 2\eta \zeta'_{(1)} \zeta_{(1)}.\tag{A.5}$$

The contribution to the bispectrum is

$$\langle \zeta(\mathbf{x}) \zeta(\mathbf{y}) \zeta(\mathbf{z}) \rangle \sim \langle \zeta_{(1)}(\mathbf{x}) \zeta_{(1)}(\mathbf{y}) \zeta_{(2)}(\mathbf{z}) \rangle + (2 \text{ perms}).$$

The first and the last terms in (A.5) are subdominant. The term quadratic in $\zeta_{(1)}$ gives contributions such as

$$\langle \zeta_{(1)}(\mathbf{x}) \zeta_{(1)}(\mathbf{z}) \rangle \langle \zeta_{(1)}(\mathbf{y}) \zeta_{(1)}(\mathbf{z}) \rangle,$$

which exist regardless of the dynamics and give $|f_{NL}| \lesssim 1$. The rest are the generic effects of the background gauge fields. Looking at (2.19), we see that the leading order contributions in \mathcal{I} are quadratic, which involve terms such as

$$\frac{\epsilon_\varphi}{\epsilon_H^3} \mathcal{I}^2 \left(2\langle \pi(\mathbf{x}) \pi(\mathbf{z}) \rangle \langle \pi(\mathbf{y}) \pi(\mathbf{z}) \rangle + \frac{1}{8} H^4 \eta^{16} \langle \alpha'(\mathbf{x}) \alpha'(\mathbf{z}) \rangle \langle \alpha'(\mathbf{y}) \alpha'(\mathbf{z}) \rangle \right)$$

and

$$\frac{\epsilon_\varphi}{\sqrt{2}\epsilon_H^3} H^2 \mathcal{I}^2 \eta^8 (\langle \pi(\mathbf{x}) \pi(\mathbf{z}) \rangle \langle \alpha'(\mathbf{y}) \alpha'(\mathbf{z}) \rangle + \langle \pi(\mathbf{y}) \pi(\mathbf{z}) \rangle \langle \alpha'(\mathbf{x}) \alpha'(\mathbf{z}) \rangle).$$

At the leading order, π and α' are essentially just $u_k(\eta)$ and $h_k(\eta)/\eta^4$, therefore their contribution will be constant of $|f_{NL}| \sim O(\mathcal{I}^2)$.

References

- [1] N. Bartolo, E. Komatsu, S. Matarrese, and A. Riotto, *Non-Gaussianity from inflation: theory and observations*, *Physics Reports* **402** (Nov., 2004) 103–266, [[0406398](#)].
- [2] J. Maldacena, *Non-gaussian features of primordial fluctuations in single field inflationary models*, *Journal of High Energy Physics* **2003** (May, 2003) 013–013, [[0210603](#)].
- [3] D. Seery and J. E. Lidsey, *Primordial non-Gaussianities from multiple-field inflation*, *Journal of Cosmology and Astroparticle Physics* **2005** (Sept., 2005) 011–011, [[0506056](#)].
- [4] D. Langlois, S. Renaux-Petel, D. Steer, and T. Tanaka, *Primordial perturbations and non-Gaussianities in DBI and general multifield inflation*, *Physical Review D* **78** (Sept., 2008) 063523, [[arXiv:0806.0336](#)].
- [5] D. Wands, *Local non-Gaussianity from inflation*, *Classical and Quantum Gravity* **27** (June, 2010) 124002, [[arXiv:1004.0818](#)].
- [6] C. Hull and P. Townsend, *Unity of superstring dualities*, *Nuclear Physics B* **438** (Mar., 1995) 109–137, [[9410167](#)].
- [7] G. W. Gibbons and K.-i. Maeda, *Black Holes in an Expanding Universe*, *Physical Review Letters* **104** (Apr., 2010) 131101, [[arXiv:0912.2809](#)].
- [8] L. Ford, *Inflation driven by a vector field*, *Physical Review D* **40** (Aug., 1989) 967–972.
- [9] T. Koivisto and D. F. Mota, *Vector field models of inflation and dark energy*, *Journal of Cosmology and Astroparticle Physics* **2008** (Aug., 2008) 021, [[arXiv:0805.4229](#)].
- [10] A. Golovnev, V. Mukhanov, and V. Vanchurin, *Vector inflation*, *Journal of Cosmology and Astroparticle Physics* **2008** (June, 2008) 009, [[arXiv:0802.2068](#)].
- [11] K. Bamba, S. Nojiri, and S. D. Odintsov, *Inflationary cosmology and the late-time accelerated expansion of the universe in nonminimal Yang-Mills- $F(R)$ gravity and nonminimal vector- $F(R)$ gravity*, *Physical Review D* **77** (June, 2008) 123532, [[arXiv:0803.3384](#)].
- [12] B. Himmetoglu, C. Contaldi, and M. Peloso, *Instability of Anisotropic Cosmological Solutions Supported by Vector Fields*, *Physical Review Letters* **102** (Mar., 2009) 111301, [[arXiv:0809.2779](#)].
- [13] T. S. Koivisto, D. F. Mota, and C. Pitrou, *Inflation from N -forms and its stability*, *Journal of High Energy Physics* **2009** (Sept., 2009) 092–092, [[arXiv:0903.4158](#)].
- [14] B. Himmetoglu, C. R. Contaldi, and M. Peloso, *Ghost instabilities of cosmological models with vector fields nonminimally coupled to the curvature*, *Physical Review D* **80** (Dec., 2009) 123530, [[arXiv:0909.3524](#)].
- [15] A. Golovnev, *Linear perturbations in vector inflation and stability issues*, *Physical Review D* **81** (Jan., 2010) 023514, [[arXiv:0910.0173](#)].
- [16] G. Esposito-Farèse, C. Pitrou, and J.-P. Uzan, *Vector theories in cosmology*, *Physical Review D* **81** (Mar., 2010) 063519, [[arXiv:0912.0481](#)].
- [17] S. Yokoyama and J. Soda, *Primordial statistical anisotropy generated at the end of inflation*, *Journal of Cosmology and Astroparticle Physics* **2008** (Aug., 2008) 005, [[arXiv:0805.4265](#)].
- [18] N. Bartolo, E. Dimastrogiovanni, S. Matarrese, and A. Riotto, *Anisotropic Bispectrum of Curvature Perturbations from Primordial Non-Abelian Vector Fields*, *Journal of Cosmology and Astroparticle Physics* **2009** (Oct., 2009) 015–015, [[arXiv:0906.4944](#)].
- [19] N. Bartolo, E. Dimastrogiovanni, S. Matarrese, and A. Riotto, *Anisotropic trispectrum of curvature perturbations induced by primordial non-Abelian vector fields*, *Journal of Cosmology and Astroparticle Physics* **2009** (Nov., 2009) 028–028, [[arXiv:0909.5621](#)].

- [20] S. Kanno, J. Soda, and M.-a. Watanabe, *Cosmological magnetic fields from inflation and backreaction*, *Journal of Cosmology and Astroparticle Physics* **2009** (Dec., 2009) 009–009, [[arXiv:0908.3509](#)].
- [21] K. Dimopoulos, M. Karčiauskas, D. H. Lyth, and Y. Rodríguez, *Statistical anisotropy of the curvature perturbation from vector field perturbations*, *Journal of Cosmology and Astroparticle Physics* **2009** (May, 2009) 013–013, [[arXiv:0809.1055](#)].
- [22] K. Dimopoulos, M. Karčiauskas, and J. M. Wagstaff, *Vector curvaton with varying kinetic function*, *Physical Review D* **81** (Jan., 2010) 023522, [[arXiv:0907.1838](#)].
- [23] C. A. Valenzuela-Toledo, Y. Rodríguez, and D. H. Lyth, *Non-Gaussianity at tree and one-loop levels from vector field perturbations*, *Physical Review D* **80** (Nov., 2009) 103519, [[arXiv:0909.4064](#)].
- [24] C. A. Valenzuela-Toledo and Y. Rodríguez, *Non-gaussianity from the trispectrum and vector field perturbations*, *Physics Letters B* **685** (Mar., 2010) 120–127, [[arXiv:0910.4208](#)].
- [25] M. Karčiauskas, *The Primordial Curvature Perturbation from Vector Fields of General non-Abelian Groups*, *Journal of Cosmology and Astroparticle Physics* **2012** (Apr., 2011) 014–014, [[arXiv:1104.3629](#)].
- [26] M. Shiraishi and S. Yokoyama, *Violation of the Rotational Invariance in the CMB Bispectrum*, *Progress of Theoretical Physics* **126** (Nov., 2011) 923–935, [[arXiv:1107.0682](#)].
- [27] T. S. Koivisto and F. R. Urban, *Cosmic magnetization in three-form inflation*, *Physical Review D* **85** (Apr., 2012) 083508, [[arXiv:1112.1356](#)].
- [28] N. Barnaby, R. Namba, and M. Peloso, *Observable non-Gaussianity from gauge field production in slow roll inflation, and a challenging connection with magnetogenesis*, *Physical Review D* **85** (June, 2012) 123523, [[arXiv:1202.1469](#)].
- [29] M. M. Anber and L. Sorbo, *Non-Gaussianities and chiral gravitational waves in natural steep inflation*, *Physical Review D* **85** (June, 2012) 123537, [[arXiv:1203.5849](#)].
- [30] R. Namba, *Curvature Perturbations from a Massive Vector Curvaton*, [[arXiv:1207.5547](#)].
- [31] F. R. Urban and T. K. Koivisto, *Perturbations and non-Gaussianities in three-form inflationary magnetogenesis*, *Journal of Cosmology and Astroparticle Physics* **2012** (Sept., 2012) 025–025, [[arXiv:1207.7328](#)].
- [32] R. K. Jain and M. S. Sloth, *On the non-Gaussian correlation of the primordial curvature perturbation with vector fields*, *Journal of Cosmology and Astroparticle Physics* **2013** (Feb., 2013) 003–003, [[arXiv:1210.3461](#)].
- [33] M. M. Anber and L. Sorbo, *Naturally inflating on steep potentials through electromagnetic dissipation*, *Physical Review D* **81** (Feb., 2010) 043534, [[arXiv:0908.4089](#)].
- [34] J. M. Wagstaff and K. Dimopoulos, *Particle production of vector fields: Scale invariance is attractive*, *Physical Review D* **83** (Jan., 2011) 023523, [[arXiv:1011.2517](#)].
- [35] E. Dimastrogiovanni, N. Bartolo, S. Matarrese, and A. Riotto, *Non-Gaussianity and Statistical Anisotropy from Vector Field Populated Inflationary Models*, *Advances in Astronomy* **2010** (Jan., 2010) 1–21, [[arXiv:1001.4049](#)].
- [36] N. Barnaby and M. Peloso, *Large Non-Gaussianity in Axion Inflation*, *Physical Review Letters* **106** (May, 2011) 181301, [[arXiv:1011.1500](#)].
- [37] N. Barnaby, R. Namba, and M. Peloso, *Phenomenology of a pseudo-scalar inflaton: naturally large nongaussianity*, *Journal of Cosmology and Astroparticle Physics* **2011** (Apr., 2011) 009–009, [[arXiv:1102.4333](#)].

- [38] N. Barnaby, E. Pajer, and M. Peloso, *Gauge field production in axion inflation: Consequences for monodromy, non-Gaussianity in the CMB, and gravitational waves at interferometers*, *Physical Review D* **85** (Jan., 2012) 023525, [[arXiv:1110.3327](#)].
- [39] K. Dimopoulos, G. Lazarides, and J. M. Wagstaff, *Eliminating the η -problem in SUGRA hybrid inflation with vector backreaction*, *Journal of Cosmology and Astroparticle Physics* **2012** (Feb., 2012) 018–018, [[arXiv:1111.1929](#)].
- [40] T. R. Jaffe, A. J. Banday, H. K. Eriksen, K. M. Górski, and F. K. Hansen, *Evidence of Vorticity and Shear at Large Angular Scales in the WMAP Data: A Violation of Cosmological Isotropy?*, *The Astrophysical Journal* **629** (Aug., 2005) L1–L4, [[0503213](#)].
- [41] T. R. Jaffe, S. Hervik, A. J. Banday, and K. M. Gorski, *On the Viability of Bianchi Type VII h Models with Dark Energy*, *The Astrophysical Journal* **644** (June, 2006) 701–708, [[0512433](#)].
- [42] T. R. Jaffe, A. J. Banday, H. K. Eriksen, K. M. Gorski, and F. K. Hansen, *Fast and Efficient Template Fitting of Deterministic Anisotropic Cosmological Models Applied to WMAP Data*, *The Astrophysical Journal* **643** (June, 2006) 616–629, [[0603844](#)].
- [43] M.-a. Watanabe, S. Kanno, and J. Soda, *Inflationary Universe with Anisotropic Hair*, *Physical Review Letters* **102** (May, 2009) 191302, [[arXiv:0902.2833](#)].
- [44] S. Kanno, J. Soda, and M.-a. Watanabe, *Anisotropic power-law inflation*, *Journal of Cosmology and Astroparticle Physics* **2010** (Dec., 2010) 024–024, [[arXiv:1010.5307](#)].
- [45] P. V. Moniz and J. Ward, *Gauge field back-reaction in BornInfeld cosmologies*, *Classical and Quantum Gravity* **27** (Dec., 2010) 235009, [[arXiv:1007.3299](#)].
- [46] R. Emami, H. Firouzjahi, S. M. S. Movahed, and M. Zarei, *Anisotropic Inflation from Charged Scalar Fields*, *Journal of Cosmology and Astroparticle Physics* **2011** (Oct., 2010) 005–005, [[arXiv:1010.5495](#)].
- [47] K. Murata and J. Soda, *Anisotropic inflation with non-abelian gauge kinetic function*, *Journal of Cosmology and Astroparticle Physics* **2011** (June, 2011) 037–037, [[arXiv:1103.6164](#)].
- [48] S. r. Hervik, D. F. Mota, and M. Thorsrud, *Inflation with stable anisotropic hair: is it cosmologically viable?*, *Journal of High Energy Physics* **2011** (Nov., 2011) 146, [[arXiv:1109.3456](#)].
- [49] T. Q. Do and W. F. Kao, *Anisotropic power-law inflation for the Dirac-Born-Infeld theory*, *Physical Review D* **84** (Dec., 2011) 123009.
- [50] T. Q. Do, W. F. Kao, and I.-C. Lin, *Anisotropic power-law inflation for a two scalar fields model*, *Physical Review D* **83** (June, 2011) 123002.
- [51] T. R. Dulaney and M. I. Gresham, *Primordial power spectra from anisotropic inflation*, *Physical Review D* **81** (May, 2010) 103532, [[arXiv:1001.2301](#)].
- [52] A. E. Gümrükçüolu, B. Himmetoglu, and M. Peloso, *Scalar-scalar, scalar-tensor, and tensor-tensor correlators from anisotropic inflation*, *Physical Review D* **81** (Mar., 2010) 063528, [[arXiv:1001.4088](#)].
- [53] M.-a. Watanabe, S. Kanno, and J. Soda, *The Nature of Primordial Fluctuations from Anisotropic Inflation*, *Progress of Theoretical Physics* **123** (June, 2010) 1041–1068, [[arXiv:1003.0056](#)].
- [54] M.-a. Watanabe, S. Kanno, and J. Soda, *Imprints of the anisotropic inflation on the cosmic microwave background*, *Monthly Notices of the Royal Astronomical Society: Letters* **412** (Mar., 2011) L83–L87, [[arXiv:1011.3604](#)].
- [55] N. Bartolo, S. Matarrese, M. Peloso, and A. Ricciardone, *The anisotropic power spectrum and bispectrum in the $f(\phi) R^2$ mechanism*, [[arXiv:1210.3257](#)].

- [56] K. Yamamoto, *Primordial fluctuations from inflation with a triad of background gauge fields*, *Physical Review D* **85** (June, 2012) 123504, [[arXiv:1203.1071](#)].
- [57] K.-i. Maeda and K. Yamamoto, *Inflationary dynamics with a non-Abelian gauge field*, *Physical Review D* **87** (Jan., 2013) 023528, [[arXiv:1210.4054](#)].
- [58] A. Maleknejad and M. M. Sheikh-Jabbari, *Non-Abelian gauge field inflation*, *Physical Review D* **84** (Aug., 2011) 043515, [[arXiv:1102.1932](#)].
- [59] A. Maleknejad, M. Sheikh-Jabbari, and J. Soda, *Gauge-flation and cosmic no-hair conjecture*, *Journal of Cosmology and Astroparticle Physics* **2012** (Jan., 2012) 016–016, [[arXiv:1109.5573](#)].
- [60] P. Adshead and M. Wyman, *Natural Inflation on a Steep Potential with Classical Non-Abelian Gauge Fields*, *Physical Review Letters* **108** (June, 2012) 261302, [[1202.2366](#)].
- [61] P. Adshead and M. Wyman, *Gauge-flation trajectories in chromo-natural inflation*, *Physical Review D* **86** (Aug., 2012) 043530, [[arXiv:1203.2264](#)].
- [62] M. Sheikh-Jabbari, *Gauge-flation vs chromo-natural inflation*, *Physics Letters B* **717** (Oct., 2012) 6–9, [[arXiv:1203.2265](#)].
- [63] E. Martinec, P. Adshead, and M. Wyman, *Chern-Simons EM-flation*, *Journal of High Energy Physics* **2013** (Feb., 2013) 27, [[arXiv:1206.2889](#)].
- [64] K. Yamamoto, M.-a. Watanabe, and J. Soda, *Inflation with multi-vector hair: the fate of anisotropy*, *Classical and Quantum Gravity* **29** (July, 2012) 145008, [[arXiv:1201.5309](#)].
- [65] R. Arnowitt, S. Deser, and C. W. Misner, *Republication of: The dynamics of general relativity*, *General Relativity and Gravitation* **40** (Aug., 2008) 1997–2027, [[0405109](#)].
- [66] K. A. Malik and D. Wands, *Cosmological perturbations*, *Physics Reports* **475** (May, 2009) 1–51, [[arXiv:0809.4944](#)].
- [67] H. Funakoshi and S. Renaux-Petel, *A modal approach to the numerical calculation of primordial non-Gaussianities*, *Journal of Cosmology and Astroparticle Physics* **2013** (Feb., 2013) 002–002, [[arXiv:1211.3086](#)].
- [68] **Planck** Collaboration, P. A. R. Ade et al., *Planck 2013 Results. XXIV. Constraints on primordial non-Gaussianity*, [arXiv:1303.5084](#).
- [69] M. Sasaki and E. D. Stewart, *A General Analytic Formula for the Spectral Index of the Density Perturbations Produced during Inflation*, *Progress of Theoretical Physics* **95** (Jan., 1996) 71–78, [[9507001](#)].
- [70] M. Sasaki and T. Tanaka, *Super-Horizon Scale Dynamics of Multi-Scalar Inflation*, *Progress of Theoretical Physics* **99** (May, 1998) 763–781, [[9801017](#)].